8-10-2022

Uncertainty quantification in climate change impacts on hydrology using three-way ANOVA

Tejith Pogakula
University of Windsor

Uncertainty quantification in climate change impacts on hydrology using three-way ANOVA

By

Tejith Pogakula

A Thesis

Submitted to the Faculty of Graduate Studies

through the Department of Civil and Environmental Engineering

in Partial Fulfillment of the Requirements for

the Degree of Master of Applied Science

at the University of Windsor

Windsor, Ontario, Canada

2022

Uncertainty quantification in climate change impacts on hydrology using three-way ANOVA

By

Tejith Pogakula

APPROVED BY:

_____

D. Ting,

Department of Mechanical, Automotive and Materials Engineering

_____

R. Seth,

Department of Civil and Environmental Engineering

_____

T. Bolisetti, Advisor

Department of Civil and Environmental Engineering

June 17, 2022

DECLARATION OF ORIGINALITY

I hereby certify that I am the sole author of this thesis and that no part of this thesis has been published or submitted for publication.

I certify that, to the best of my knowledge, my thesis does not infringe upon anyone's copyright nor violate any proprietary rights and that any ideas, techniques, quotations, or any other material from the work of other people included in my thesis, published or otherwise, are fully acknowledged in accordance with the standard referencing practices. Furthermore, to the extent that I have included copyrighted material that surpasses the bounds of fair dealing within the meaning of the Canada Copyright Act, I certify that I have obtained a written permission from the copyright owner(s) to include such material(s) in my thesis and have included copies of such copyright clearances to my appendix.

I declare that this is a true copy of my thesis, including any final revisions, as approved by my thesis committee and the Graduate Studies office, and that this thesis has not been submitted for a higher degree to any other University or Institution.

ABSTRACT

Climate change impact modelling studies utilize an ensemble of climate model projections obtained from various Regional Climate Models (RCM). These climate projections, extracted under different emission scenarios (representative concentration pathways) are then bias-corrected using observed meteorological data and the resulting bias-corrected projections are forced through a hydrological model in order to assess the climate change impacts on future streamflow. Uncertainties arise from various sources like inputs, model structure, model parameters, choice of hydrological model, choice of climate models, bias correction, etc. along every step of the impact assessment study. Quantifying such uncertainties and further assessing the contribution of each factor under consideration leads the modellers to draft robust climate change adaptation and management policies.

The aim of this Thesis is to quantify and decompose the uncertainty contribution of three factors namely choice of Climate Model (CM), Representative Concentration Pathways (RCP) and Bias Correction Methods (BCM), and the uncertainties arising out of their factor interactions toward the total uncertainty using Analysis of Variance (ANOVA). To this extent, five sets of Climate Models (CM), two different emission scenarios (RCP 4.5 and RCP 8.5) and two non-linear bias correction methods were used in conjunction with the Soil & Water Assessment Tool (SWAT) hydrological model for the headwater catchment of Little River Experimental Watershed in Georgia, USA. The results indicate the overall and seasonal uncertainty decomposition, and it is evident from the results that Climate Model choice (CM) is the biggest contributor toward the total uncertainty in this modelling process.

Keywords: Regional Climate Models, bias correction, uncertainty, SWAT model, Analysis of Variance (ANOVA)

DEDICATION

To my beloved parents, brother and to God.

ACKNOWLEDGEMENTS

I would like to thank my parents and my brother for their never-ending emotional and financial support and commitment towards my graduate study.

I am honestly thankful for the enormous support and resources which my supervisor Dr. Tirupati Bolisetti has contributed for my MASc study. I will be forever grateful for his guidance over the course of my study and especially appreciate him for being the strongest emotional support during some personal mental and physical health complications during the COVID-19 pandemic.

I acknowledge United States Department of Agriculture – Agricultural Research Service for providing recently archived databases for flow and climate data among other necessary data for the Little River Experimental Watershed.

I sincerely acknowledge the program reader, Dr. Rajesh Seth and the outside program reader, Dr. David Ting for their valuable time and providing extremely important feedback and suggestions to improve the quality of the research.

I would like to take this opportunity to specially thank PhD graduate, Dr. Vinod Chilkoti for his time and efforts in imparting his knowledge in hydrological models and uncertainty modelling.

I am also greatly appreciative and thankful to my fellow research colleague Rahul Narula for his continuous help in conceptualizing and solving "R" coding problems. The continuous and available support was one of the strongest technical lifelines I have had over the period of my MASc study.

Finally, I would like to thank my fellow graduate students Kiran, Saranya, Afanur and Israt for their continuous support.

TABLE OF CONTENTS

LIST OF TABLES

LIST OF FIGURES

CHAPTER 1: INTRODUCTION

1.1 Background

The Intergovernmental Panel on Climate Change (IPCC) defines climate change as the change in the condition of the climate that can be detected by performic statistical study on the mean and/or variability of its attributes over time, generally decades or more (IPCC, 2001). The variation in climate over time, whether caused by natural variability or human activity, is referred to as climate change. Climate change has been at the forefront of the most challenging issues to the environment in recent years and there is an incessant need to gain an enhanced knowledge of how the changing climate will affect the hydrological processes around the world. This requirement is even more profound in case of understanding the streamflow projections. Over the last decade, studies investigating the uncertainty induced during streamflow forecasting using future climate forcings have grown increasingly common in the hydrologic literature. There is a huge problem in perfectly grasping the enormous spectrum of uncertainty that comes with our understanding of climate change (Kim et.al, 2019). Decisions we make now could have long-term consequences decades from now because of the timescales inherent in climatic and economic systems. Most decision-analysis systems recommend a policy based on the best-estimated future predictions (Lempert et.al, 1996).

Global climate change has already been shown to have long-term consequences on water resources that will last far into the next century (Bosshard et al., 2013). For decision makers, future streamflow estimates provide a significant foundation for assessing various hydrological extremes, such as floods and droughts (Giuntoli et al., 2018) on water management decisions. This information is useful for developing effective countermeasures for a changing climate (Addor et al., 2014). As a result of the high level of uncertainty in these climate change estimates, the

decision for suitable adaptation policies can be challenging (Whateley and Brown, 2016). Hence, in climate change impact studies, recognizing and quantifying projection-related uncertainty is critical.

Climate change projections are prone to uncertainties mainly because of three factors: uncertainty in scenario, model uncertainty, and climate variability within the system (Deser et al., 2010). Scenarios are representative concentration pathways like RCP4.5 and RCP8.5 and refer to the hypothetical, long-term situations wherein the changes in greenhouse gas emissions, short-lived species and land-use-land-cover stabilize the radiative forcing at 4.5 and 8.5 Watts per metre squared, respectively. General circulation models (GCMs) are one of the main instruments for simulating how the global climate system will respond to rising levels of greenhouse gas (GHG) emissions and for making predictions about the future climate projections. GCMs are sophisticated mathematical models of the physical and dynamical processes that govern and drive the hydrological cycle. With the increasing complexity of a climate model, the higher the model accuracy and consequently, the higher is the computational prowess required. GCMs use a spatial grid with a coarse resolution in order to reduce the computational workload, which can be a considerable strain (IPCC, 2001). In case of finer scale climate impact studies, GCM projections cannot be directly used due to the scale requirements. Because of this resolution mismatch, statistical and dynamical downscaling techniques have been widely used. Recent studies show that bias correction has limited downscaling abilities, even if the scale difference is small (for instance, when using values averaged over watersheds) (Maraun, 2016). Dynamic downscaling, on the other hand, employs the use of high-resolution climate models known as regional climate models (RCM) which are computationally intensive models generated through using the projections from coarser-resolution climate models, namely GCMs as boundary conditions. The RCM projections obtained

from the Coordinated Regional Climate Downscaling Experiment (CORDEX) are used to assess the climate change impacts. These RCMs are of 0.22-degree resolution, implying a grid size of roughly 25 km * 25 km.

The climate projection outputs from RCMs have inherent biases which need to be corrected before using the climate forcings onto the hydrological model. Different bias correction techniques are available to perform this task. Bias correction can be a simple linear or the more sophisticated non-linear type. Linear bias correction methods employ a constant factor to add or multiply the RCM projections with, to bias correct the future data based on the difference or ratio between the observed and modelled data over a reference/historical period. Non-linear bias correction consists of trend-preserving operations performed on the modelled climate projections based on the quantile distributions and additional trends of both observed and modelled data over the reference period.

In order to understand climate change impacts on hydrological processes, it is imperative to first understand the hydrologic cycle. (Donnelly et al., 2017). The hydrologic cycle is defined as the continuous water circulation and its interactions across various phases of nature i.e. atmosphere, land surface, open water, subsurface, etc. (Bedient et al., 2008). Hydrology in watersheds is affected by climate change, and this needs to be modelled using accurately calibrated and validated models with various climate scenarios to get a more solid estimate of uncertainty (Li et al. 2016). Some hydrological models can also predict agricultural productivity and river sediment under diverse land use scenarios and management scenarios over a long span of time in the future, while taking a historical time-period as the reference period.

Uncertainty can be defined as the state of limited knowledge or data where it is not possible to perfectly describe an existing state or future outcomes. Uncertainty can arise out of various

sources like output uncertainty, input uncertainty, hydrological model uncertainty, climate model uncertainty, parameter uncertainty and parameter uncertainty. Uncertainty can be of two types namely, aleatoric/statistical uncertainty and epistemic/systemic uncertainty. Epistemic uncertainty stems out of incomplete understanding and representation of model structures, hydrological phenomena and parameters while aleatoric uncertainty stems from the probabilistic variations in any random event. Uncertainty is inherent in any prediction. Understanding the nature of the uncertainties and quantifying them will facilitate for robust climate change adaptation policies. Ignoring uncertainties is bound to conceal risks, in turn misrepresenting the climate change impacts. Uncertainty is one of the biggest challenges in the development of adaptation plans and needs to be carefully addressed. Quantifying and expressing in numbers and percentage, the uncertainty contribution of each source in the modelling process towards the total uncertainty is known as uncertainty decomposition. It may also include the contributions of uncertainty due to interactions between the sources.

The uncertainty propagation in any climate change impact assessment framework needs to be thoroughly investigated. Understanding the nature of the uncertainties and quantifying them will make it easier to develop robust climate change adaptation plans in the future. Prior studies used statistical models like GLUE (Beven and Binley, 1992), SUFI-2 (Abbaspour et al., 2007a), Monte-Carlo simulation (Wilby and Harris, 2006), cumulative distribution function analysis (Chen et al., 2010), variable control approach (Dobler et al., 2012), variance decomposition (Datta et al., 2013), signal-to-noise ration (Thober et al., 2018) were used to quantify uncertainty arising from different factors but such methods failed to consider the interactions between the factor levels. In this study, analysis of variance (ANOVA) statistical technique is used to achieve uncertainty decomposition. Using the ANOVA method, the total

variance of the predicted values is divided into components attributable to each individual sources and to the interactions between them.

Most of the prior uncertainty assessment studies considered decomposing uncertainty of only one simple flow metric like mean flow or median flow. However, the uncertainty decomposition varies across different segments of a flow duration curve and therefore, there is a need to consider extreme (low & high flows) and a representative metric (mean flow). Breaking down the uncertainty arising due to factor interactions has only been explored in a very limited number of studies. Disregarding the further uncertainty breakdown between interactions obscures the actual importance of a factor (uncertainty source).

1.2 Objectives of the study

The main objective of this research is:

> To identify and decompose, the uncertainties arising from three sources namely, emission scenarios (RCP), bias correction methods (BCM) and climate models (CM) and their interactions by using a 3-way ANOVA while employing the use of mean flow (Q_{mean}), low flow (Q_5) and high flow (Q_{95}) streamflow metrics.

To this end, a SWAT hydrological model for the study area will be developed and water budget analysis will be performed. The same model will be analysed for parameter sensitivity before it is calibrated and validated.

1.3 Structure of the Thesis

This Thesis is divided into 5 chapters. The introductory chapter provides background information about climate change, bias correction, hydrological modelling and uncertainty decomposition. Chapter 2 contains the review of literature on the study area, hydrologic modelling, climate change impacts, uncertainty assessment and ANOVA. Chapter 3 consists of detailed description of the data and methodology used in the study for SWAT modelling, bias correction and 3-way ANOVA. Results and discussions on SWAT model, climate change impacts and ANOVA are presented in Chapter 4. Final remarks and conclusions along with suggestions for future work are all presented in the last Chapter 5.

CHAPTER 2: LITERATURE REVIEW

This chapter provides an insight into the review of prior literature for Little River experimental watershed, SWAT model, climate change impacts, uncertainty assessment and ANOVA framework.

2.1 Little River Experimental Watershed

Little River Experimental Watershed (LREW) is a 334 sq.km watershed located in the Georgia coastal plains. It is one of the experimental watersheds monitored by the US Department of Agriculture-Agricultural Research Service Southeast Watershed Research Laboratories (SEWRL). Multiple studies have been performed on LREW and its sub watersheds since the 1980s (Sheridan et al., 1995; Shirmohammadi et al., 1986; Sheridan and Hubbard, 1987). In the recent years, Bosch et al., (2004) compared SWAT and BASINS model in simulating the total maximum daily loads (TMDLs). An investigation was undertaken to observe and compare the performing capabilities and drawbacks of manual calibration to those of three automatic calibration methods (SSQauto6, SSQRauto6 and SSQauto11), of the SWAT model for the LREW (M.W. Van Liew et al., 2005). Changes in land use and conservation practices and their impacts on watershed hydrology was studied for 34 years of hydrologic data over LREW (Bosch et al., 2006). Long term climate, flow, sediment data, etc. databases were generated for the purpose of water-quality study of the streamflow, impact studies of changes in LULC and management practices, soil studies, etc. (Bosch et al., 2007). Long-term water chemistry database for chloride, nitrogen, phosphorus, etc. was prepared for the 8 sub watersheds of LREW (Feyereisen et al., 2007). Sahoo et al., (2008) conducted performance evaluation to gauge the reliability of NASA's Advanced Microwave Scanning Radiometer (AMSR-E) soil moisture data by comparing it with in-situ data at the LREW. Cho et al., (2010) studied the effect of dividing sub watersheds on the SWAT model simulation

for the LREW. The effect of the most predominant conservation practices namely, tillage conservation and slope positioning on the watershed hydrology was studies (Bosch et al., 2012). Multiple water balance components like surface runoff, evaporation and groundwater flow were integrated for constraining multi-objective calibration for an improved performance of the SWAT model (Pfannerstill et al., 2017). Pisani et al., (2020) studied the influence of riparian land cover on the dissolved organic matter in the predominantly agricultural watershed of LREW. Hydrologic characteristics of the data intensive LREW were compared to those of surrounding watersheds to check if the former is representative of coastal plain watersheds (Bosch et al., 2021). Choudhary and Athira, (2021) studied the effect of soil moisture on the surface and subsurface SWAT model simulations for LREW.

2.2 Hydrological Model (SWAT Model)

Hydrological models try to schematise the dynamic workings of the flow of water within the hydrological cycle. Models use basic laws such as conservation of mass and energy as well as Newton's laws to represent (to a fair extent) the mathematical relationships between the dynamics of natural hydrological cycle. It is imperative to note that no model in existence ca simulate nature and its phenomenon fully because of the various complexities in nature. Hydrological models can be divided into lumped (HyMod), semi-distributed (SWAT) and fully distributed (MIKE-SHI) based on spatial discretization. Lumped models have only one unit representing the whole watershed, whereas the semi-distributed model has multiple units (HRUs in case of SWAT) to represent a single watershed and the modelling processes are simulated differently for each of these units. Fully distributed or distributed models have their watershed represented by a uniform-sized grid. The modelling complexity and time increase from lumped to fully distributed. Based on the complexity of process description, models are classified into empirical (SVM, ANN),

conceptual (HyMod, NAM) and Physical (SWAT, MIKE-SHI). Oftentimes choosing a suitable model for a study involves considering the trade off between model complexity and the computational power required to run the model. SWAT is a continuous model which implies that it can be used for modelling a series of values over a given time period for the considered time scale (daily, monthly, etc) but it cannot be used to simulate a single event. SWAT is physically based signifying that it required actual ground data representation like topography (DEM), soils and land cover inputs apart from the climatic variable inputs. Prior to the SWAT2012 hydrological model used in this study, there were a various use cases of simpler and more versions of SWAT model some of which are as follows: ESWAT included an automatic calibration routine and was used for performing sub-daily water quality studies (Griensven and Bauwens, 2001); SWAT-G had improved transpiration mechanics and was used for modelling mountainous watersheds in Germany (Eckhardt et al., 2002); SWIM included key hydrological processes at both smaller and larger (> 10,000 sq. km) basin levels (Krysanova et al., 2005).

Arnold et al. (2012) reviewed calibration and validation techniques, most sensitive parameters for different components of water budget, pollutants and nutrients. It also provided detailed description of steps to be followed for calibration and uncertainty analysis.

2.3 Climate Change Impacts

Climate change impacts arise out of the interactions between climate change and the vulnerability of an exposed system. Climate change impacts affects various sectors like decrease crop yield, lower nutritive quality, and increased crop diseases in agricultural sector; Increased erosion, high flooding risk to coastal settlements in infrastructure sector; Decline in steady water availability for hydropower generation impacting hydropower sector (Chilkoti, 2019). Studying the impacts of climate change on extremes is of utmost importance for sustainable ecosystem and

social functioning. Climate change and population increase have become major stumbling blocks to long-term natural resource conservation. Extreme features like floods and droughts should not be purely attributed to "natural hazards" because anthropogenic interventions strongly influence drought features (Haile et al., 2020). The impact of climate change on the environment and society grows in lockstep with global warming (Touma et al., 2015). Similarly, climate change has been shown to have a significant impact on global hydrological systems, with its consequences continuing into the next century (Bosshard et al., 2013; Addor et al., 2014). Future streamflow forecasts provide a useful foundation for assessing various hydrological extremes (Giuntoli et al., 2018), which help in formulating effective climate-change responses (Addor et al., 2014). Any climate change impact study will involve the following steps, namely hydrological model calibration and validation followed by forcing the extracted future climate forcings, after bias corrections, onto the hydrological model to obtain and assess the climate change impacts. The uncertainty arising in such climate change impact modelling process is our primary focus in this thesis. Figure 2-1 depicts the steps in a typical climate change impact modelling study.

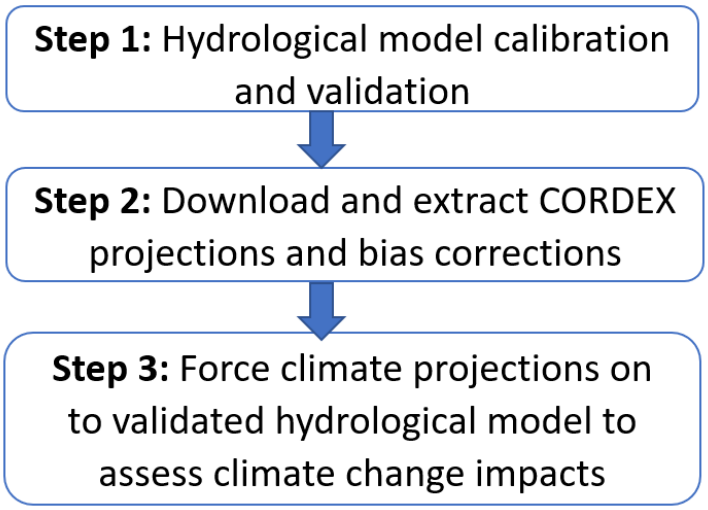

Figure 2-1: Climate change impact modeling chain

2.4 Uncertainty Assessment

The focus of this study is mainly on climate model uncertainty, uncertainty due to RCP scenarios and uncertainty due to bias correction methods and their interactions but this section presents a brief overview of uncertainty assessment for multiple sources. Input uncertainty, climate model uncertainty, simplification of the underlying physical processes, output uncertainty, hydrological model and parameter uncertainty all contribute to the overall uncertainty in the climate change modelling process (Beven, 2016; Athira and Sudheer, 2015). Uncertainty is inherently present in the modelling process because of the sources and hence their identification and subsequent quantification is on the forefront of challenges faced by hydrologic modellers (Beven and Freer, 2001). Different climate change impact studies were performed identifying and quantifying various factors as uncertainty contributors such as choice of climate model (Arnell, 2011; Chen et al., 2011; Dobler et al., 2012; Karlsson et al., 2016; Chegwidden et al., 2019; Zhang et al., 2020; Her et al., 2019), hydrological model (Arnell, 2011; Karlsson et al., 2016; Wang et al., 2020; Tarek et al., 2021, Zhang et al., 2021), bias correction methods (Aryal et al., 2019; Wang et al., 2020), land-use scenarios (Karlsson et al., 2016), hydrological parameters (Chilkoti, 2019; Zhang et al., 2021), RCP scenarios (Wilby and Harris, 2006; Vetter et al., 2017; Chegwidden et al., 2019; Stojkovic et al., 2020) among many other factors like internal variability (Deser at al., 2012), choice of precipitation datasets and initial conditions, downscaling techniques, etc.

Datta, (2011) presented an intensive review of mainstream traditional uncertainty assessment techniques which were being employed for a modelling study. The earlier uncertainty assessment method–type 1 operated under the assumption that every uncertainty source/factor can be explained by means of parameter uncertainty. GLUE (Beven and Binley, 1992) and Sequential

Uncertainty Fitting (SUFI-2) algorithm are two Bayesian techniques that fall under this category. GLUE generates many random parameters sets and runs simulations within a model structure and then retains the "behavioural" parameter sets and provides a likelihood measure based on posterior distribution matching. SUFI-2 presents the parameter uncertainty as a multivariate uniform distribution wherein the model parameters are calibrated to conform so that most of the measured data points are encompassed by the 95 PPU band (Abbaspour et al., 2004, 2007).

Uncertainty quantification related to the output is ascertained by employing the use of the statistical error models which show a bias in parameter estimation. Such biases, therefore simultaneously affect the parameter uncertainty and prediction uncertainty too (Schoups and Vrugt, 2010; Thyer et al., 2009). In cases where the model residuals are correlated (Laloy et al., 2010; Schaefli et al., 2007; Yang et al., 2007a,b; Bates and Campbell, 2001; Duan et al., 1988; Kuczera, 1983; Sorooshian and Dracup, 1980), the correlations are removed by means of autoregressive (AR) models. Engeland et al., (2010) employed the use of Normal Quantile Regression in conjunction with AR model to achieve the same while factoring in the non-normality of the residuals.

These primitive types of uncertainty assessment methods were limited in the sense that the individual effects of different sources of error on the model predictions cannot be isolated. To overcome this flaw, UA method-type 3 were introduced wherein different sources of uncertainty like input uncertainty, model structure uncertainty and parameter uncertainty could be isolated and individually accounted for. To assess the input, output and model structure uncertainty, the BATEA framework (Kavestki et al., 2006a) was employed (Renard et al., 2010). Vrugt et al., 2003 suggested the use of Shuffled Complex Evolution Metropolis (SCEM–UA) an optimization algorithm and further developed the Differential Evolution Adaptive Metropolis (DREAM)

algorithm (Vrugt et al., 2008) for stronger optimisation of parameters to better represent error models with complex, multimodal target distributions. The simultaneous parameter optimization and data assimilation method (SODA) (Vrugt et al., 2005) was used to quantify different sources of uncertainty namely input, output, parameter and model structure uncertainties in the modelling process by making a representative stochastic model of the deterministic hydrological model and use parameter estimation to explain the state estimation. SODA was an advanced algorithm which encompassed the parameter search efficiency of the SCEM-UA method and computational efficiency of the ensemble Kalman filter.

Predictive uncertainty and Variance Decomposition (VD) technique was used to quantify the uncertainty contribution of parameter uncertainty as a fraction of the total uncertainty in order to improve the reliability of predictive uncertainty (Datta et al., 2013). Yip et al., (2011) used the ANOVA framework to decompose the uncertainty in global mean surface temperature arising out of model uncertainty, scenario uncertainty and internal variability. ANOVA is superior to the variance decomposition method (Datta et al., 2013) because it considers the uncertainty arising out of interaction between the factors or sources while the latter ignores it when in actuality, interaction terms contribute to total uncertainty as per prior literature. In recent years, ANOVA framework has been increasingly used for uncertainty analysis and decomposition because of its ease of use and capability to quantify even the uncertainty arising out of interaction of sources.

2.5 ANOVA

The uncertainty propagation in any climate change impact assessment framework needs to be thoroughly investigated. Understanding the nature of the uncertainties and quantifying them will make it easier to develop robust climate change adaptation plans in the future. In this study,

analysis of variance (ANOVA) (Von Storch and Zwiers (2001, chapter 9)) statistical technique is used to achieve uncertainty decomposition. Using the ANOVA method, the total variance of the predicted values is divided into components attributable to each individual sources and to the interactions between them (Kim et al., 2019). According to Yip et al. (2011), the entire uncertainty in the surface air temperature prediction was split into uncertainties arising from natural variability, emission scenarios as well as GCMs and their interactions. The analysis of variance method (ANOVA) was employed by Bosshard et al. (2013) to determine the uncertainty contributions of global climate models, downscaling methodologies, hydrological model choice, and their interactions. Gaur et al. (2021) performed ANOVA to quantify uncertainty due to RCM, RCP scenarios, RCM-RCP interaction and Internal Variability and presented that internal variability has a considerable part of total variance. Meresa et al. (2022) performed a 3-way ANOVA between GCM, hydrological parameters and emission scenarios and concluded that GCM is the biggest contributor to uncertainties in extreme flows. Lee et al. (2022) studied the effect of hydrological model, climate simulation and bias correction methods and ascertained that hydrological models had the most contribution to total uncertainty for low flows over a Korean watershed. Tarek et al (2021) performed a 3-way ANOVA to study uncertainty of rainfall datasets in comparison to other factors namely hydrological models and GCMs and found that the choice in precipitation datasets contributed to about 10-20% of the total uncertainty. Troin et al. (2018) used a four-way ANOVA with seven snow models, five potential evapotranspiration techniques, three hydrologic models, and two ensemble members to quantify and breakdown the uncertainty of hydrological forecasts in two Canadian Nordic Quebec watersheds. Hydrological models were determined to be the primary source of uncertainty. For the Pacific Northwest, Chegwidden et al. (2019) used a four-way ANOVA with two emission scenarios, ten GCMs, two downscaling approaches, and two

hydrological models to quantify and breakdown the uncertainty of hydrological forecasts in the area. This research demonstrated that the emission scenarios and GCMs were substantial contributors to the variation of annual streamflow volume uncertainty. In a similar manner, Dakhlaoui et al. (2022) performed a 3- way ANOVA between 11 climate models, 3 hydrological models and 2 emission scenarios for five Northern Tunisian watersheds and concluded that climate model choice was the dominant source of uncertainty. Zhang et al. (2021) performed a 5-way ANOVA between GCMs, hydrological models, model parameters, emission scenarios and bias correction methods and found that GCM is the leading contributor to uncertainty. Lemaitre-Basette et al. (2021) performed a slight variation of ANOVA known as QE-ANOVA to study uncertainty decomposition of 5 factors and found that GCM choice is the major contributor by a huge margin.

CHAPTER 3: METHODOLOGY

Chapter 3 summarizes the data and methodology used in this study. It consists of a brief overview of study area, climate profile, GIS, meteorology and flow, and climate projections input data, and the methodology of hydrological model, bias correction methods and ANOVA framework.

3.1 Study area

The Little River Experimental Watershed (LREW) with an area of 334 km^2, which is located in the Southern Atlantic Coastal Plains near Tifton in Georgia, USA is selected for this study (Figure 3-1). The LREW is situated in the upper reaches of the Suwannee River basin and was established by the United States Department of Agriculture-Agricultural Research Service (USDA-ARS) to offer hydrologic, soil and natural resource data to be used for monitoring and research purposes (Cho et al., 2010. LREW consists of a flat topography with gently ascending (2-5% slope) uplands. The predominant land use in the watershed are woodlands (50%), row crops (31% - with majority of the crop yield being peanut and cotton employing the use of crop rotation), pasture (10%) and water bodies (about 2%). The underlying soil formations are mostly made up of Tifton loamy sand (36%) followed by Alapaha loamy sand (12%) and other types of finer sandy loam soils (Wyatt et al., 2020). The predominant soil in this region, sandy loam has a high infiltration rate of about 5 cm/hr (Choudhary and Athira, 2021). The streamflow generation itself ranges between 30-40% of the yearly precipitation (Rajat and Athira, 2021). About 80% of the total streamflow is the lateral flow rejoining the streams through shallow aquifers rather than the direct surface runoff itself which accounts to about 20% of it (STEWARDS). From prior research of the LREW watershed, direct overland flow accounts for about 5-40% while shallow sub-surface flow accounts for about 2-35% of the total annual precipitation over the watershed (Bosch et al., 2012).

The headwater catchment considered for the current study is an upstream part of the LREW with an area of 50 km^2 and consists of LRI, LRJ, LRM and LRK sub-watersheds as depicted by Figure 3-1.

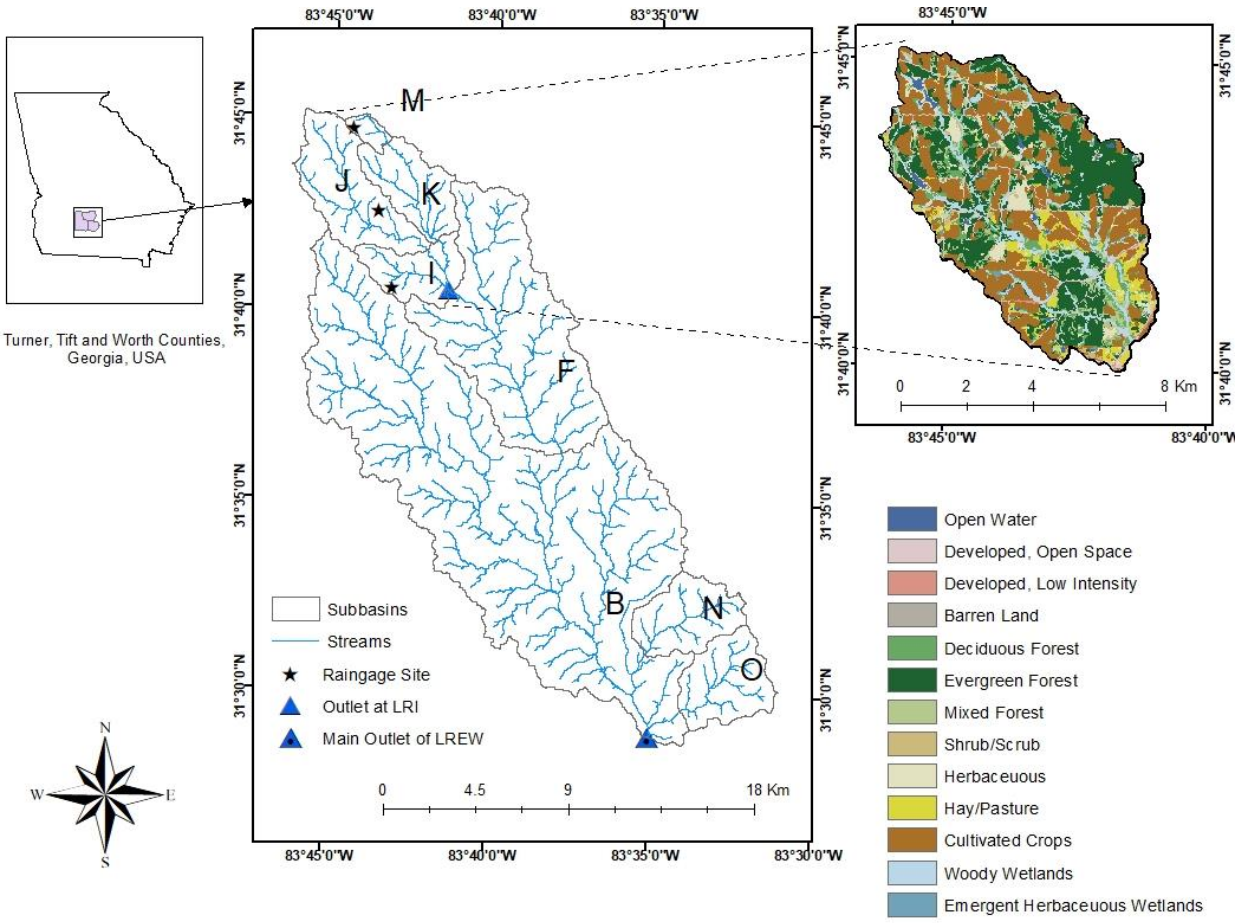

Figure 3-1: Study Area: Headwater catchment of Little River Experimental Watershed (LREW) in Georgia, USA

3.2 Climate profile

The climatic profile of LREW is humid subtropical with average of 1200 mm of precipitation every year. The annual average temperature is 18.7 ^{o}C, with mean monthly temperatures varying between 10.6 ^{o}C for the coldest month of January and 26.8 ^{o}C for the hottest month of July.

Precipitation events throughout the summer indicate lesser depths, decreased duration, greater intensity, and higher frequency of when compared to the rest of the seasons of the year (Bosch et al., 2017). The rainfall is scanty and unevenly distributed over the watershed which causes ephemeral streamflow, i.e., there is no continuous streamflow within the reaches and there are often no-flow days, especially during the dry seasons).

3.3 Input data

3.3.1 GIS data

The spatial data prerequisites for the study area consist mainly of Digital Elevation Model (DEM), land use and soil data layers and other miscellaneous layers like stream shape layer and watershed boundary. The 30 m resolution USGS DEM available as National Elevation Datasets for the study area was obtained from USGS TNM download website (https://apps.nationalmap.gov/downloader/#/). The land use data layer was downloaded for the National Land Cover Database 2011 (NLCD) from the data gateway website of USDA (https://datagateway.nrcs.usda.gov/). The Soil Survey Geographic (SSURGO) database soils data layer was obtained from Natural Resources Conservation Service (NRCS) website (https://websoilsurvey.sc.egov.usda.gov/). The watersheds, stream shapefiles were obtained from from Sustaining the Earth's Watersheds–Agricultural Research Data System (STEWARDS) website (https://www.nrrig.mwa.ars.usda.gov/stewards/stewards.html).

3.3.2 Meteorological data and flow data

Daily precipitation and temperature data are the two main weather inputs required in the specific study. There are other weather inputs, such as wind velocity, humidity, solar radiation,

etc., required to simulate the hydrologic cycle. There are 43 rain gauges spread out over the study area out of which 31 rainfall gauges are still operational.

The SWAT model used the precipitation data for 3 rain gauges (Figure 3-1) which were obtained from Sustaining the Earth's Watersheds–Agricultural Research Data System (STEWARDS) website (https://www.nrrig.mwa.ars.usda.gov/stewards/stewards.html) and the archived Tifton website (http://radio.tiftonars.org/archived_data.html) provided by USDA-ARS. The temperature data, both maximum and minimum temperature, available from 1911 – 2022, for Ashburn and Tifton stations closest to the study area from the National Oceanic and Atmospheric Administration (NOAA) are accessed from their website (https://www.ncei.noaa.gov/). The missing temperature data from Ashburn is filled in using Multiple Imputation by Chained Equations (MICE) using Tifton data for missing data correlation and imputation.

The missing data for precipitation were filled using simple arithmetic mean method for the station. The reason for choosing arithmetic mean method is because of the criteria of the 30-year annual climate normals of surrounding stations being within the range of 10% of the considered station with missing data. The 30-year climate normals were obtained using the PRISM satellite dataset of 800 x 800 m^2 resolution obtainable from the PRISM climate group website (https://prism.nacse.org/).

There are eight streamflow measuring stations in the study area operational. The daily observed streamflow data from 1968 – 2018 were obtained from Sustaining the Earth's Watersheds–Agricultural Research Data System (STEWARDS) website (https://www.nrrig.mwa.ars.usda.gov/stewards/stewards.html). There are four flow gauging

stations within the study area, each one corresponding to the outlet of the four subbasins (Figure 3-1).

The flow data from 1974-2003 was subset for the flow gauging station at the outlet at LRI **(**Figure 3-1**)** namely GALR4950. Missing data was filled as a mean of preceding and succeeding values of the missing date wherever applicable.

3.3.3 Climate projection data

All climate models used in this study were part of the Coordinated Regional Climate Downscaling Experiment (CORDEX) obtained from the CORDEX website (https://esg-dn1.nsc.liu.se/search/cordex/). The climate projections, both historical and future for two representative concentration pathways (RCPs) as described in Table 3-1 are used. Regional Climate Models (RCMs) of 25 x 25 km^2 were used for the North American domain (NAM-22) for extracting projected data for each climate model. A total of five RCM – General Circulation Model (GCMs) combinations were extracted under RCP 4.5 and RCP 8.5 emission scenarios for historical period (1983 - 2012) and future period (2070-2099).

Table 3-1: The 5 climate models used for the study

No.	RCM	Resolution (Km)	Driving GCM	Scenarios
1	CCCma-CanRCM4	25	CCCma-CanESM2	RCP 4.5, RCP 8.5
2	OURANOS-CRCM5	25	CCCma-CanESM2	RCP 4.5, RCP 8.5
3	OURANOS-CRCM5	25	CNRM-CERFACS-CNRM-CM5	RCP 4.5, RCP 8.5
4	OURANOS-CRCM5	25	MPI-M-MPI-ESM-LR	RCP 4.5, RCP 8.5
5	OURANOS-CRCM5	25	NOAA-GFDL-GFDL-ESM2M	RCP 4.5, RCP 8.5

3.4 Methodology

The methodological framework opted for assessing the climate change impacts for this study is presented in Figure 3-2. For this purpose, the step-wise propagation of uncertainty throughout the modelling process is taken into account encompassing five Climate Models (CM), two Representative concentration Pathways (RCP) and two non-linear Bias Correction Methods (BCM) for a total of 5x2x2 combinations. A single precipitation dataset (GALR dataset), for modelling and bias correcting, and a semi-distributed hydrological model (SWAT) are used for this uncertainty decomposition study since the focus is on uncertainty contribution from the CM, RCP and BCM on the impacts of climate change. From the prior literature, it is evident that the choice of climate model is one of the biggest sources of uncertainty (Prudhomme et al., 2013).

Hydrological modeling, bias correction and uncertainty analysis are described in detail in the following sections.

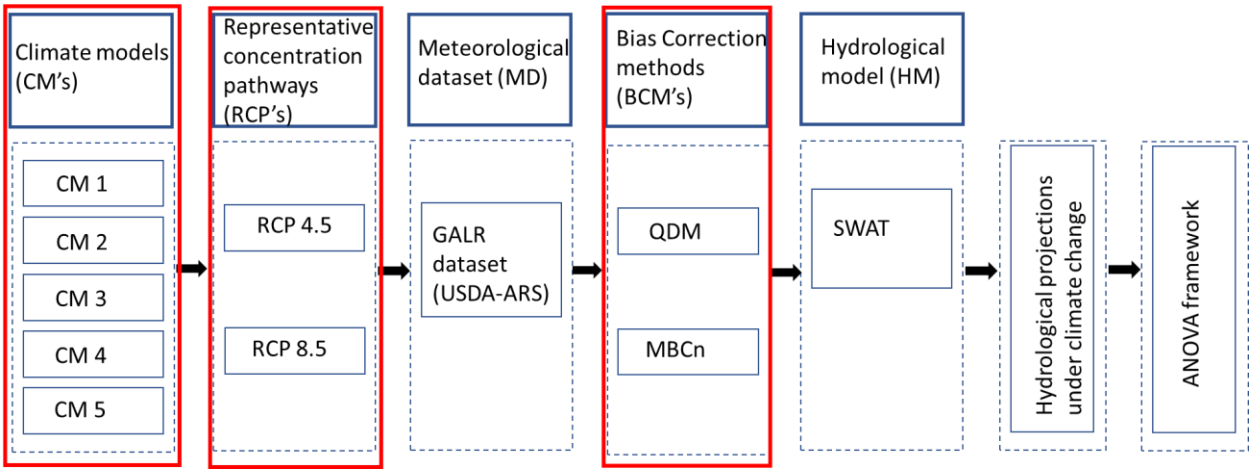

Figure 3-2: Framework for the methodology proposed for the study

3.4.1 Hydrological Model

Soil and Water Assessment Tool (SWAT) is a semi-distributed hydrological model developed by Dr. Jeff Arnold for the USDA ARS. It is a widely used robust model which is capable of simulating continuous processes of the watershed hydrology like streamflow and sediment transportation. The model requires climatic and geographical variables too because SWAT is a physically based model. Once the input variables are entered into the model, SWAT performs water balance calculations at the required timescale (daily, monthly, etc). This step is followed by sensitivity and the regionalization of parameters for calibration and validation of the model and subsequent performance evaluation, which if deemed necessary is then used to run the simulations to obtain the required output (Streamflow, ET, etc.). Figure 3-3 presents the framework of SWAT hydrological model.

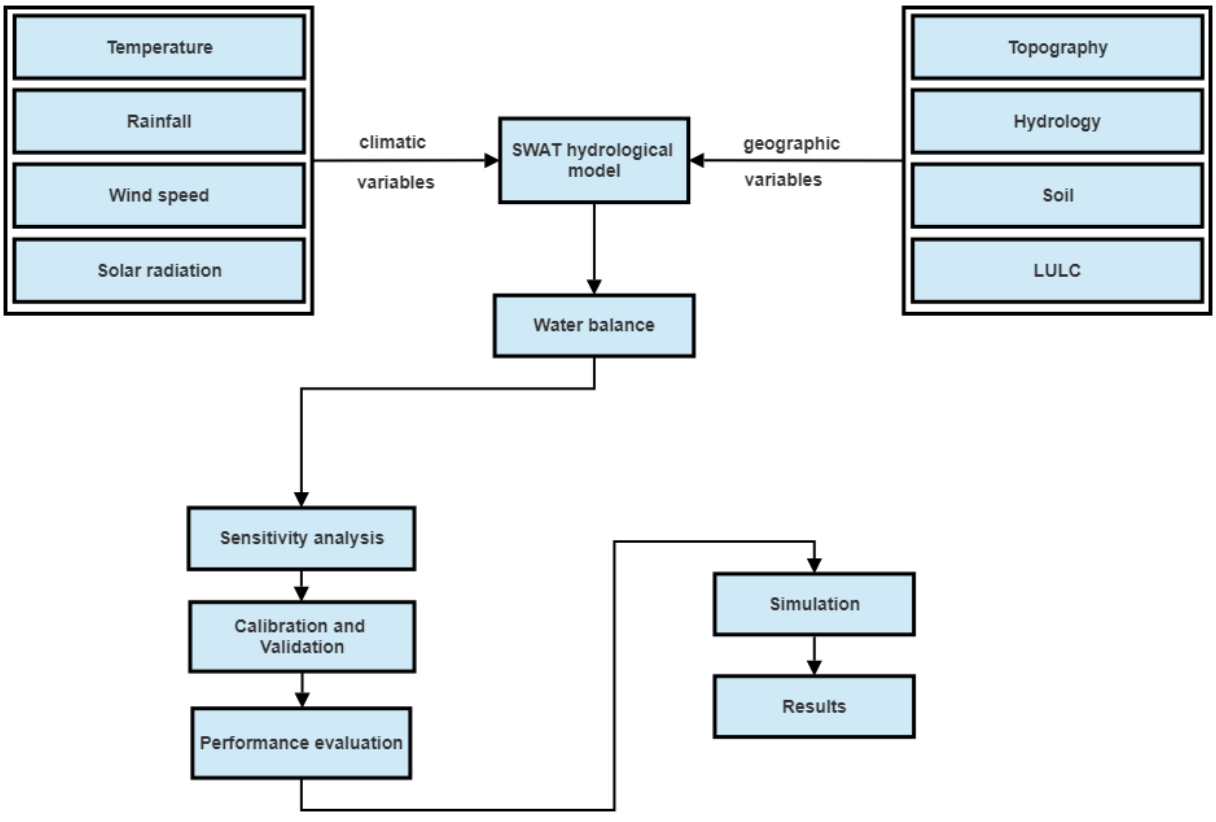

Figure 3-3: Operational framework of SWAT hydrological model

QSWAT (QGIS interface) was used to delineate the study area into 4 sub-basins and the sub-basins were further broken down into 73 HRUs (Hydrological response units) based on 5% threshold criteria for the slope, land use and soils.

Initially, global sensitivity was run for 25 parameters out of which 9 parameters (CN_2, SOL_AWC, GW_REVAP, ALPHA_BF, SLSUBBSN, CH_K2, OV_N, SOL_K, HRU_SLP) were sensitive. But for the sake of consistency, a set of 15 parameters, with an additional 6 parameters from prior literature were used for the calibration process. Baseflow.exe program provided by the SWAT TAMU official website was used for baseflow separation and the resulting value of Alpha was used for ALPHA_BF initiation.

Table 3-2: The SWAT model parameters and their calibrated values

Parameters	Description	Unit	Range type	Min	Max	LREW
CN2_F	Curve Number	%	r	-0.25	0.25	-0.14625
SOL_AWC	Soil available water capacity	%	r	-0.3	0.3	0.6425
SOL_K	Soil saturated hydraulic conductivity	%	r	-0.25	0.25	0.06375
SURLAG	Surface runoff lag coefficient	–	a	0.1	10	4.6045
ESCO	Soil evaporation compensation factor	–	a	0.01	1	0.24265
EPCO	Plant uptake compensation factor	-	a	0	1	0.131667
HRU_SLP	Average slope steepness	%	r	-0.5	1	0.5625
SLSUBBSN	Average slope length	%	r	-0.5	0.5	0.241667
OV_N	Manning's 'n' for overland flow	%	r	-0.1	0.3	0.924833
GW_DELAY	Delay time for aquifer recharge	Days	a	0	500	75.83333
GW_REVAP	Groundwater revap coefficient	–	a	0.02	0.2	0.1937
GWQMN	Threshold water level in shallow aquifer for baseflow	mm H20	a	0	2000	1436.667
ALPHA_BF	Baseflow recession constant	1/days	a	0	1	0.268333
CH_K2	Effective hydraulic conductivity in main channel alluvium	mm/hr	a	0.1	150	52.31517
SOL_BD	Moist bulk density	%	r	-0.06	0.06	-0.0198

The SWAT model is set up for the 11-year period of 2005-2015. Calibration period is set to be from 2005-2010 and 2011-2015 is set as the validation period with a 3-year warm-up period. SWAT CUP is used for calibration of the model for the watershed. Table 3-2 encompasses the SWAT model parameters used for calibration in this study. SWAT parameters can range among different scales like reach scale (e.g., CH_K2), HRU scale (e.g., CN2, ESCO, EPCO, etc.) and watershed scale (eg. GW_REVAP, GWQMN, etc.). The symbols 'r' and 'a' denote relative (percentage-based) and absolute(replacement) changes respectively.

3.4.1.1 Model evaluation

Nash-Sutcliffe Efficiency (NSE), Percentage Bias (PBIAS) and Kling Gupta Efficiency (KGE) are the performance metrics to evaluate the hydrological model performance. These metrics are defined as follows:

$$NSE = 1 - \frac{\sum_{i=1}^{n}(Q_o - Q_s)^2}{\sum_{i=1}^{n}(Q_o - Q_{o(avg)})^2} \quad \text{(Eq. 3-1)}$$

Wherein Q_o is observed discharge, Q_s is simulated discharge and $Q_{o(avg)}$ is the average of all the observed discharge values and n is the number of observations. NSE ranges between -∞ to 1, where the closer to 1 it is, the perfect the simulation is. An NSE value > 0.5 is considered acceptable for SWAT model monthly flow simulation. NSE metric is sensitive to extremes, particularly discharge peaks. To overcome this limitation, it is used in conjunction with KGE which is less sensitive to the peaks which is expressed as below:

$$KGE = 1 - \sqrt{(r-1)^2 + (\frac{Q_{sSD}}{Q_{oSD}} - 1)^2 + (\frac{Q_{s(avg)}}{Q_{o(avg)}} - 1)^2} \quad \text{(Eq. 3-2)}$$

Wherein *r* is the Pearson Correlation Coefficient, Q_{sSD} and Q_{oSD} are the standard deviations of the simulated and observed discharges respectively and $Q_{s(avg)}$ is the average of all the simulated discharge values. KGE value measures the Euclidian distance components corresponding to correlation, bias, and variability from the ideal point. KGE value also ranges from -∞ to 1, where 1 represents a perfect simulation. It is expressed as follows:

$$r = \frac{\sum_{i=1}^{n}(Q_o - Q_{o(avg)})(Q_s - Q_{s(avg)})}{\sqrt{\sum_{i=1}^{n}(Q_o - Q_{o(avg)})^2}\sqrt{\sum_{i=1}^{n}(Q_s - Q_{s(avg)})^2}} \quad \text{(Eq. 3-3)}$$

And finally, PBIAS measures the net overestimation or underestimation of values by the model. A PBIAS value of 0% indicates perfect estimation of simulated values by the model when compared to the observed values. A value between -20% to 20% is considered acceptable for SWAT monthly model.

$$PBIAS = \frac{\sum_{i=1}^{n}(Q_s - Q_o)}{\sum_{i=1}^{n} Q_0} \times 100 \quad \text{(Eq. 3-4)}$$

3.4.2 Bias correction

The climate data projections modeled by the General Circulation Models (GCMs) or the finer Regional Climate Models (RCMs) have innate biases due to a multitude of reasons like inability to perfectly replicate hydrological processes of nature (Maraun, 2012). These modeled climatic simulations have biases which are evident when compared to the ground-based observational data. Bias correction techniques are applied to correct the projected data for such biases. These techniques often consist of a deriving an equation or a function to represent the empirical distributions for climate projections for a control period (historical period with observed data) to map and conform with the empirical distributions of the observed dataset for the same period. This correction function is subsequently applied to the future climate projections of the models.

Bias correction methods of different types have their own pros and cons ranging from simple linear bias correction (like linear scaling) to non-linear bias correction methods (like

Quantile Mapping). Non-linear bias correction methods are further classified into Univariate bias correction where only one climate variable can be corrected at one time and multivariate bias correction wherein multiple climate variables like precipitation at different extraction points are bias corrected simultaneously. One univariate bias correction method namely Quantile Delta Mapping (QDM) method is used in the present study. The QDM method (Cannon et al., 2015) employs the use of quantiles to correct for the biases between the observed and modelled historical data and project the biases onto future modelled data. Usually, an additional function would be required to project the change in quantiles over the historical period into the future period. QDM bypasses this requirement using a two-step framework, wherein firstly the quantiles of the future model projections are detrended so that they can overlap the historical period and then the change in quantiles between the observed and modelled historical series' quantiles is used to bias correct the detrended future projections.

This study also uses a multivariate bias correction approach through Multivariate Bias Correction N-PDF transform (MBCn) for simultaneously correcting multiple ratio variables like precipitation, taking into account their interactions (Cannon, 2018). In this method, a random orthogonal rotation is applied to both source (modelled) and target (observed) data before QDM is used to correct the marginal distributions of the rotated source data. In this case, the QDM is applied not directly to each variable independently but to a linear combination of the original climate variables under consideration. Lastly, the corrected dataset is rotated back using inverse rotation and it is compared to the unchanged target data. This framework is repeated over multiple iterations for better fitting and bias correction. One hundred iterations were chosen to conduct the specific study. Figure 3-4 presents a brief overview of the steps involved in both QDM and the MBCn bias correction methods.

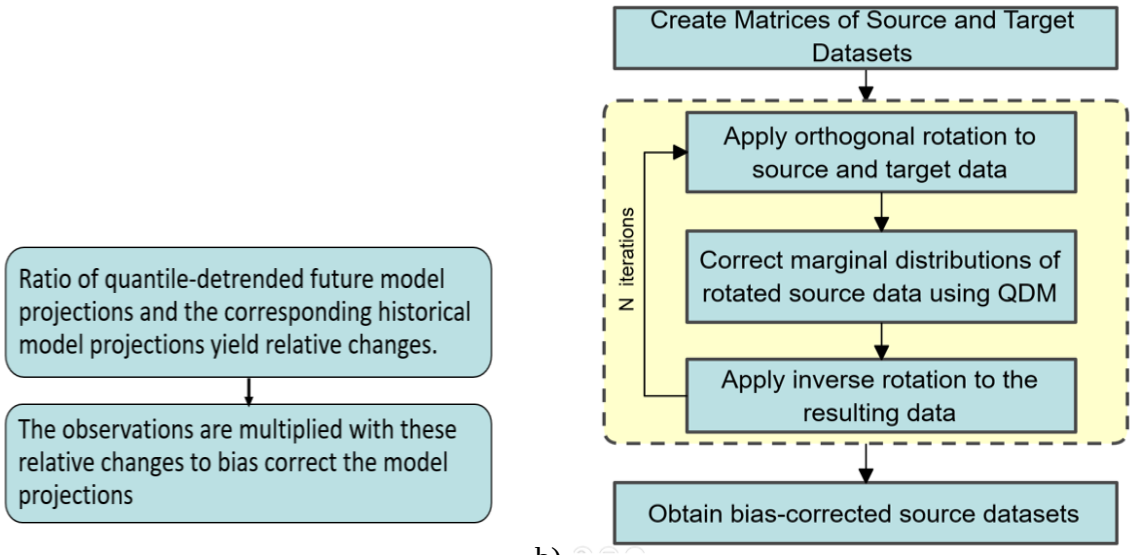

a) b)

Figure 3-4: Framework of a) Quantile Delta Mapping (QDM) and b) Multivariate Bias Correction N-pdf transformation (MBCn) methods of bias correction

3.4.3 ANOVA framework

The stagewise layout of the framework from Figure 3-2 makes it evident that different choices in each step cause a total of 5x2x2 (20) different hydrologic simulations for the estimation of uncertainty and its decomposition into source contributions for the considered climate change impact study. Monthly mean streamflow (Q_{mean}), low flows (Q_5) and peak flows (Q_{95}) are the hydrological metrics used for the uncertainty assessment in this study.

Analysis of Variance (ANOVA) is a statistical technique employed for breaking down total uncertainty into uncertainty arising out of various sources and their interactions (Wang et al., 2020). Interaction between sources is considered to show the variance caused by the sources which do not behave linearly. For instance, the variance between modelled streamflow metric because of multivariate bias correction of the climate models might be much lower than in case of bias

correcting with a univariate method and vice versa. ANOVA also facilitates sub-sampling of sources and allows us to observe in-depth the sub-sampled 2-way interactions between the sources.

Assumptions of an ANOVA study:

1) Dataset is normally distributed
2) Data in each group is independent of the other
3) Variance within each group is more or less the same

The three uncertainty components under consideration for this study (CM, RCP and BCM) leads to the computation of 7 variance components namely 3 main effect components, 3 first-order components (2-way interactions) and 1 second-order component (3-way interaction) which can be shown as below:

$$U_{Total} = U_{RCM} + U_{BCM} + U_{RCP} + U_{RCM:BCM} + U_{RCM:RCP} + U_{RCP:BCM} + U_{RCM:BCM:RCP} \quad \text{(Eq. 3-5)}$$

The f-test performed along during ANOVA signifies the importance of each factor towards the total uncertainty by means of the p-values obtained from their corresponding f-values. The result of the ANOVA test is statistically significant when the p-value is greater than the chosen threshold (commonly taken as 0.05) which implies that at least one group (factor) differs from the other and the study will require further steps to quantify such effects. To quantify the percentage contributions of uncertainty from each source and interactions, variance measure (eta squared) η^2 is used. It is obtained from the ratio of sum of squares of the component to the sum of squares of total uncertainty and η^2 varies between 0 indicating 0% contribution to total uncertainty and 1 indicating a 100% contribution (Bosshard et al., 2013). To this end, the uncertainty decomposition

results are presented in the form of bands of variances for each factor, measured by η^2 expressed in percentage.

CHAPTER 4: RESULTS AND DISCUSSIONS

4.1 General

Chapter 4 presents the results and discussions for the present study. This chapter covers the model calibration and validation, including parameter sensitivity analysis followed by climate model projections for temperature and precipitation followed by bias correction. Climate change impacts are then presented as sensitivity of evapotranspiration to the temperature changes and as streamflow sensitivity as a result of precipitation changes followed by analysis of flow duration curves and water budget analysis for the study are for end century period. Lastly, Uncertainty decomposition due to ANOVA is presented as overall variance, monthly variance with interacting factors and a visual depiction of the interactions of the factors.

4.2 Calibration and validation of hydrological model

SWAT modeling process involves many parameters. Using all the available parameters is ineffective as it consumes enormous time and computational resources and most of the parameters are not sensitive or influential to the changes in outputs. For calibrating and validating the model using SUFI-2 algorithm, we first need to select the parameters to run the SWAT-CUP iterations. Based on the previous literature, a set of twenty-five parameters were initially considered and global sensitivity analysis was performed which resulted in the parameters being limited to nine sensitive parameters. For the sake of consistency and brevity with prior studies on LREW, a set of fifteen parameters were selected, adding six more parameters to the highly sensitive parameters (CN_2, SOL_AWC, GW_REVAP, ALPHA_BF, SLSUBBSN, CH_K2, OV_N, SOL_K, HRU_SLP). The t-stat and the p-value of the chosen parameters are presented in Table 4-1**.**

Table 4-1: Sensitivity analysis for the selected parameters

Parameter Name	t-Stat	P-Value	Sensitivity
SCS runoff curve number (CN2)	31.76	0	HIGH
Available water capacity of the soil layer (SOL_AWC)	14.63	0	HIGH
Groundwater "revap" coefficient (GW_REVAP)	6.89	0	HIGH
Baseflow alpha factor (ALPHA_BF)	-6.88	0	HIGH
Average slope length (SLSUBBSN)	4.41	0	HIGH
Effective hydraulic conductivity in the main channel (CH_K2)	3.56	0	HIGH
Manning's "n" value for overland flow (OV_N)	3.42	0	HIGH
Soil conductivity (SOL_K)	-2.82	0.005	HIGH
Average slope steepness (HRU_SLP)	-2.21	0.028	HIGH
Threshold depth of water in the shallow aquifer required for return flow to occur (GWQMN)	1.73	0.085	MEDIUM
Soil evaporation compensation factor (ESCO)	-1.72	0.086	MEDIUM
Groundwater delay (GW_DELAY)	-1.03	0.305	LOW
Plant uptake compensation factor (EPCO)	0.91	0.361	LOW
Surface runoff lag time (SURLAG)	-0.81	0.416	LOW
Soil moist bulk density (SOL_BD)	0.26	0.793	LOW
Threshold depth of water in the shallow aquifer required for "revap" flow to occur (REVAPMN)	0.17	0.863	LOW

SWAT model was calibrated and validated using the Sequential Uncertainty Fitting (SUFI-2) algorithm of SWAT-CUP program. From the prior literature review, a list of 15 model parameters presented in Table 4-1 were chosen to calibrate and validate the SWAT model. The parameter sets were optimized after 3 iterations of 500 runs each. Model calibration and validation were performed at the outlet gauge GALR 4950 of the LRI watershed. The Figure 4-1 corresponds to the time series of Observed Vs Simulated monthly flows for the calibration and validation period.

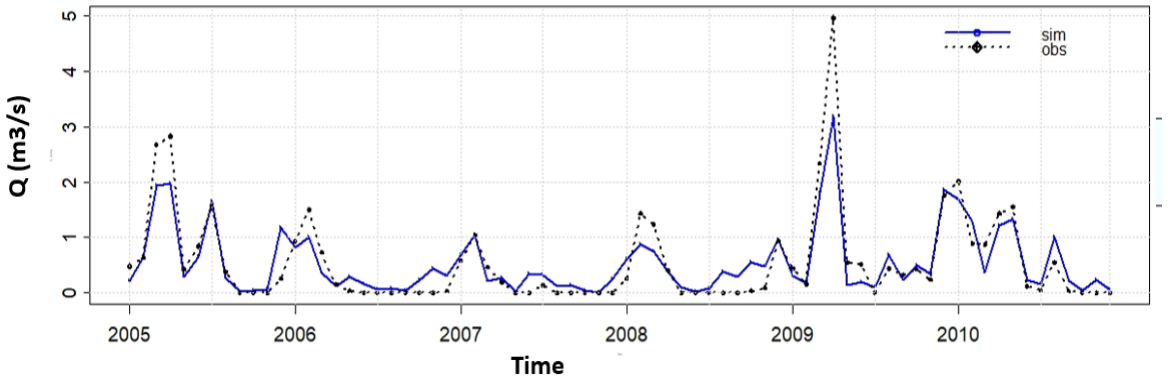

a)

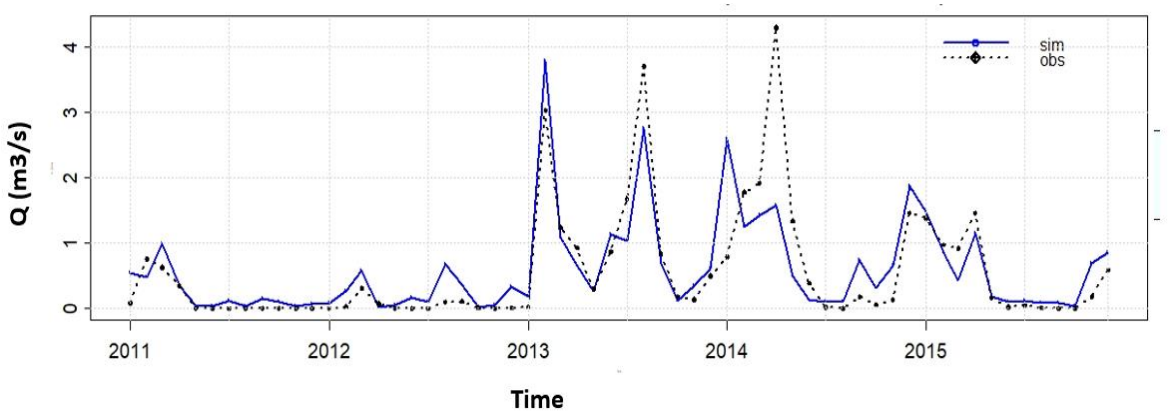

b)

Figure 4-1: Observed VS simulated streamflow hydrographs for a) Calibration and b) Validation periods

The SWAT model was calibrated for a period of six years, from 2005 to 2010. The observed Vs simulated plot depicted in Figure 4-1 a) is used for qualitative evaluation while three objective functions, namely NSE, KGE and PBIAS are used for quantitative evaluation. From Figure 4-1 a), there is an overall good agreement between the observed and simulated flows excluding a few months. Simulated flows were higher for certain months like November 2005, November 2006, November 2007, August, September, October, November 2008. This seasonal overprediction during the winter corresponds to the precipitation during those months with zero streamflow measured. The model consistently underpredicted the flow corresponding to huge peaks like the ones corresponding to March, April 2005, February, March 2008, April 2009. This might be attributed to the model overpredicting the soil available moisture content, while lowering the actual value of the curve number. The performance metric values for the calibration period at the outlet were NSE = 0.82, KGE = 0.70 and PBIAS = 1.7. A positive value of PBIAS indicates the overestimation of simulated streamflows for the calibration period.

The SWAT model was validated for a period of five years, from 2011 to 2015. The observed Vs simulated plot depicted in Figure 4-1 b) is used for qualitative evaluation while three objective functions, namely NSE, KGE and PBIAS are used for quantitative evaluation. There is a good overall correlation between observed and simulated values except for a few months. Simulated flow was visibly higher for the month of July 2012, February 2013 and January 2014 and lower during the months of July 2013, continuous period of February, March, April, May of 2014. The overprediction of simulated flows are in correspondence to high values of precipitation. For instance, the precipitation measured for January 2014 was over 180 mm, but the observed flow was less than 1 m^3/sec. The continued lower simulation covering the spring 2014 might be a random modeling occurrence attributed to failure of the model in accurately predicting the lateral

flow, which is mostly parameterized by baseflow, groundwater delayed flow and ESCO parameters. For the validation period, the performance measures were NSE = 0.65, KGE = 0.73 and PBIAS = - 5.3. The negative PBIAS value in this case indicates the overall underestimation of streamflows during the validation period.

Table 4-2 indicates the performance evaluation criteria of calibration and validation period according to Moriasi et al., (2015) and Kouchi et al., (2017).

Table 4-2: Performance evalation for calibration and validation period

Period	Objective Function	Value	Performance Evaluation
Calibration (2005-2010)	NSE	0.82	Very Good
	KGE	0.7	Satisfactory
	PBIAS	1.7	Very Good
Validation (2011-2015)	NSE	0.65	Satisfactory
	KGE	0.73	Satisfactory
	PBIAS	-5.3	Good

4.3 Climate model projection

The rise in harmful greenhouse gas emissions and CO_2 levels causes the radiative forcing of the earth to increase. Radiative forcing is the net energy flux retained by earth's atmosphere, measured in Watts per square metre. This increase in the net energy flux causes change in climatic conditions like increased temperatures and increased severity of storms among other adverse changes. For this Thesis, two separate emission scenarios/representative concentration pathways were considered namely RCP 4.5 and RCP 8.5 corresponding to net energy flux of 4.5 Watts/m^2 and 8.5 Watts/m^2 respectively. This section presents the changes in temperature and precipitation for the end-century period followed by bias correction for mean precipitation for the same.

4.3.1 Temperature projections

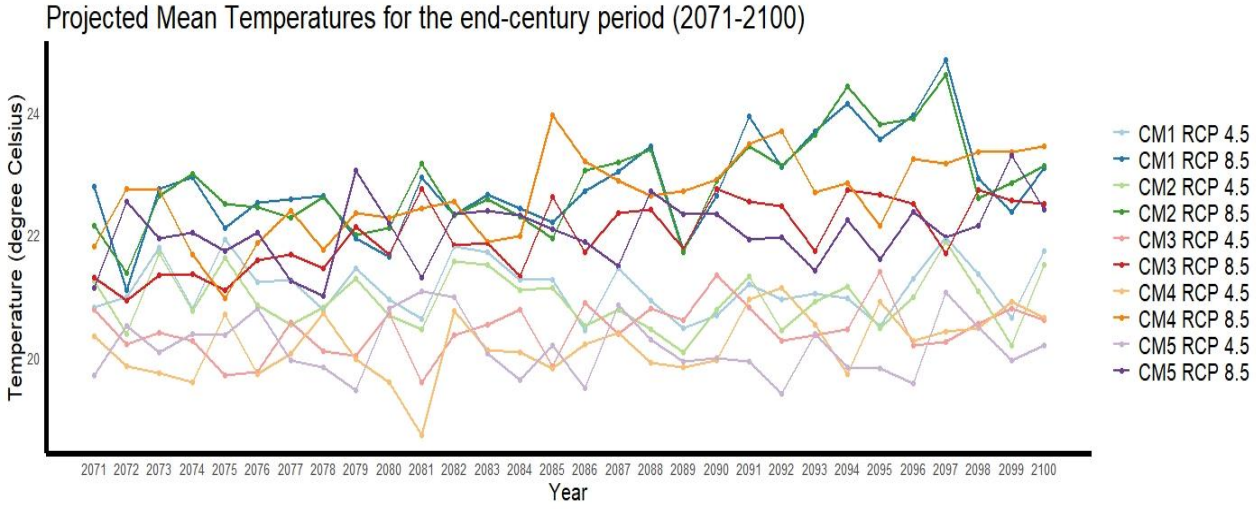

Figure 4-2: Projected Mean Temperatures for the end century period (2071-2100)

Figure 4-2 corresponds to the temperature increase under RCP 4.5 and 8.5 scenarios over the end century period (2071-2100) for the watershed wherein different climate models are illustrated using different colour with the lighter shade indicating RCP 4.5 while the darker shade indicates RCP 8.5 respectively. From the figure, it is evident that CM1 and CM2 have good correlation among the five climate models. The other climate models have significant variations in projecting the mean annual temperatures for the end century period causing a widely spread ensemble of model projections. There is a mean increase of up to 0.6 degrees Celsius from 2071 to 2100 for the temperature projection ensemble spread. Increased temperature projections indicate increased dry spells and/or increased evapotranspiration as a result.

4.3.2 Precipitation projections

a)

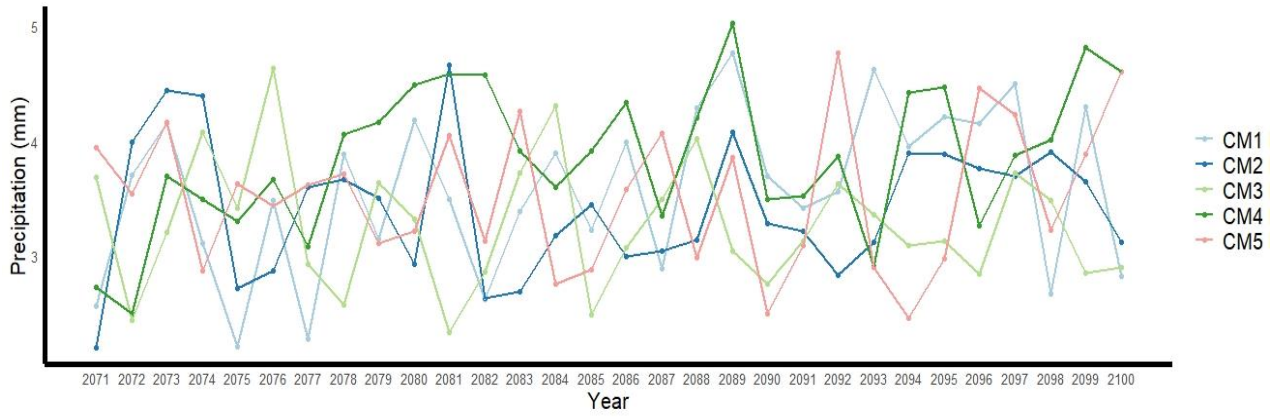

b)

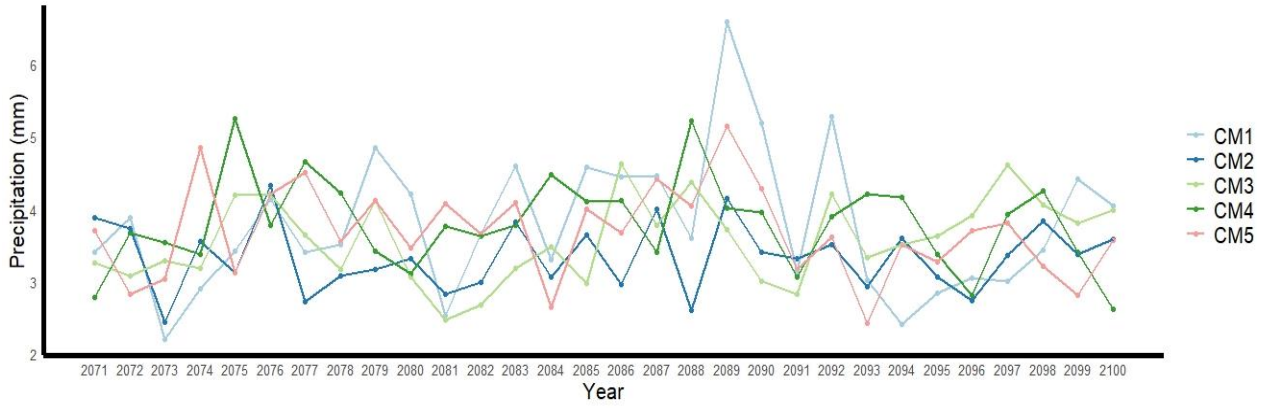

Figure 4-3: Projected mean precipitation for the end century period under a) RCP 4.5 and b) RCP 8.5 emission scenario

Global warming causes warmer oceans and an increase in evaporation into the air causing more intense storms. In this section, the precipitation projections are presented for two different emission scenarios, namely RCP 4.5 and RCP 8.5 for the end-century period (2071-2100). From Figure 4-3, it is evident that none of the climate models have good correlation among themselves. The ensemble of model projections forms a wide band, which goes to prove that the choice of climate model selection has a large effect on precipitation projections. The modeled precipitation

ensemble shows a sudden increase near the year 2089 indicating the occurrence of an extreme precipitation (with high intensity rainfall and/or large return period) event in that year.

4.3.3 Bias correction

The climate model simulated outputs so not conform statistically to the observed data for the control period and have some inherent biases. These biases arise out of various reasons like incomplete conceptualization of natural phenomena, discretization, parameterisations, reanalyses, etc. which need to be corrected before proceeding with the climate change impact assessment. Bias correction is a prerequisite for correcting future model projections based on the observed historical data. Many studies only consider univariate bias correction techniques like linear scaling, quantile mapping wherein the climatic variables like temperature and precipitation are bias-corrected independently. But in actuality, temperature and precipitation are correlated (Tarek et al., 2021). To prevent improper representation of the climate data for the impact assessment framework, this Thesis considers one univariate (Quantile Delta Mapping) and one multivariate (Multivariate Bias Correction – N pdf Transformation) bias correction method.

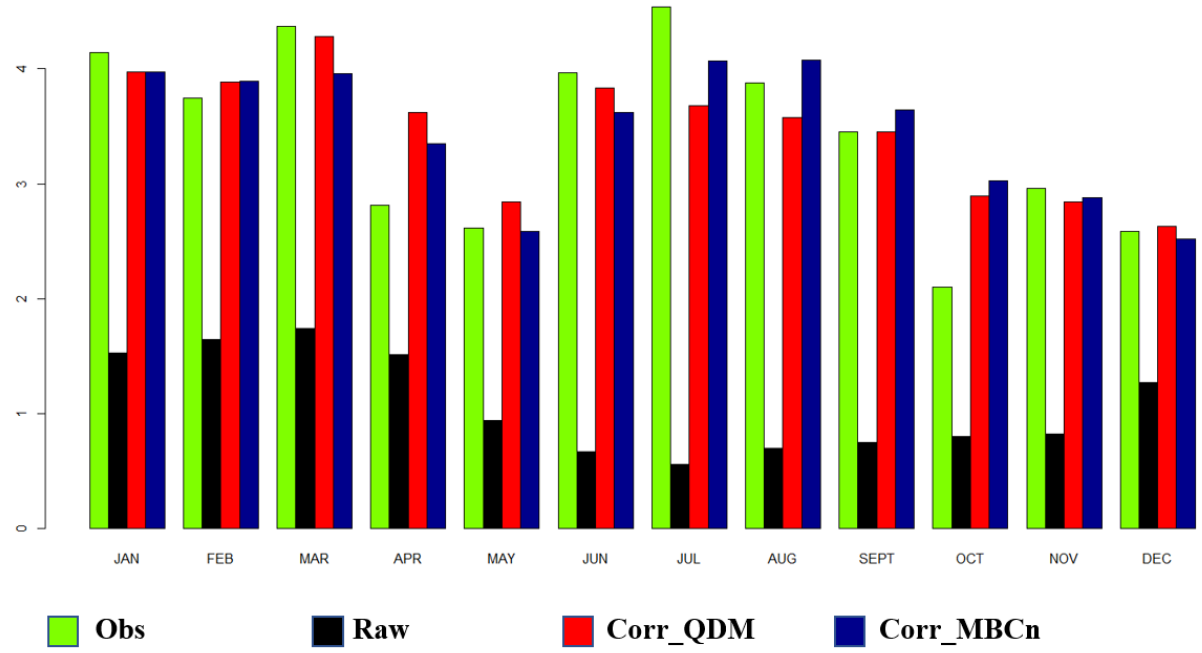

Figure 4-4: Observed, raw and QDM and MBCn bias corrected precipitation data

Initially, the raw data of future simulations is vastly different as compared to that of the observed historical data. This shows the presence of biases in the climate model precipitation and temperature data. Figure 4-4 depicts the observed, raw and bias-corrected average monthly values for both Quantile Delta Mapping and Multivariate Bias Correction N-pdf transformation methods. The graph illustrates the huge bias in raw and observed values. The raw model projections were severely under predicting the precipitation values. The bias-corrected values are closer to the actual observed values after applying both non-linear bias correction methods. This reinforces the fact that bias correction must be done before proceeding to the next steps in a climate change impact assessment study.

4.4 Climate change impacts

Climate change impacts are the consequences of climate change occurring across various sectors. Climate change has adverse effects like hotter temperatures, rise in oceanic levels, scarcity of food, loss of species, droughts among many others affecting many sectors. This Thesis emphasizes climate change impacts on hydrology. Generally, climate change causes an unnatural speeding up of the hydrological cycle. Warmer temperatures lead to higher rates of evaporation and transpiration and precipitation itself by increasing convectional currents. This section assesses the impacts of climate change on hydrology by observing the changes in hydrological components such as evapotranspiration, streamflow and/or the water budget itself.

4.4.1 Evapotranspiration

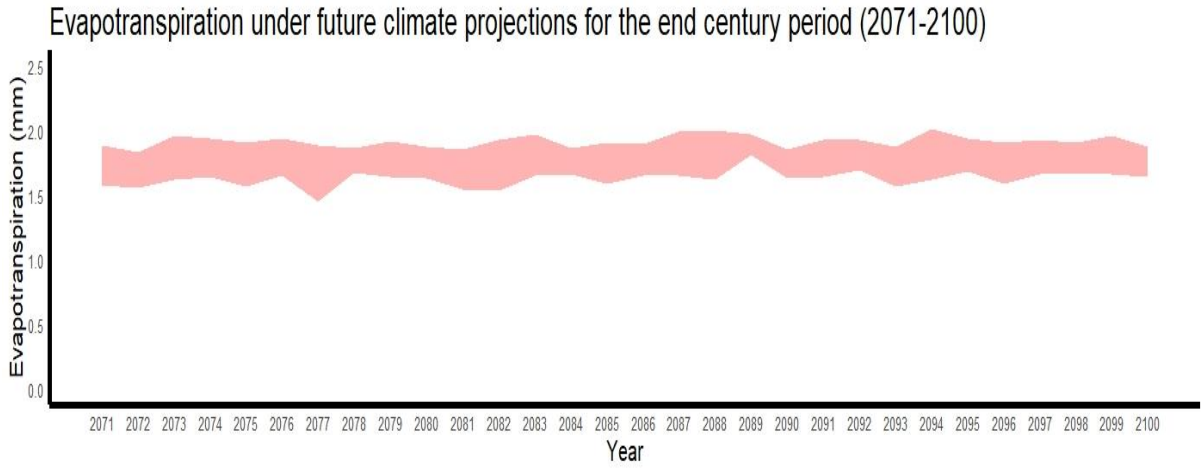

Figure 4-5: Ensemble for model projections of evapotranspiration for the end century.

Due to global warming, there is a rise in evapotranspiration which subsequently indicates the redirecting a portion of precipitation that is supposed to run off as surface flow or infiltrate into the subsurface as groundwater recharge. Evapotranspiration projections presented in Figure 4-5 show a narrow ensemble band for the ET projections which implies that ET sensitivity to

temperature is relatively lower. Regardless of the sensitivity, it is evident that in accordance with the temperature projections from Figure 4-2, ET projections also follow an upward, increasing trend. For an average 0.6 degrees Celsius increase of temperature between 2071-2100, ET relatively increases by a small degree of around 0.1 mm based on the trendline slope.

4.4.2 Streamflow climate sensitivity

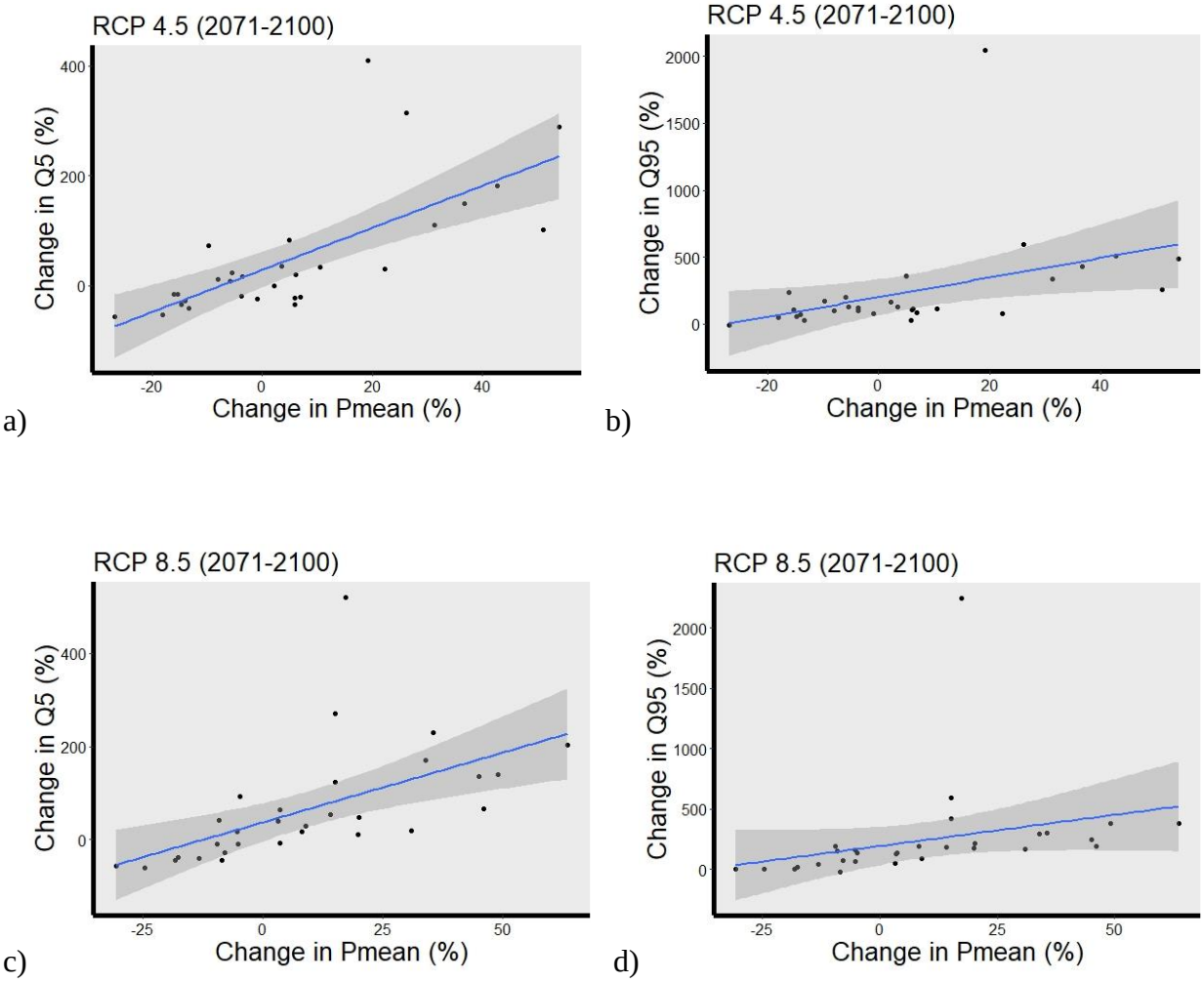

Figure 4-6: Streamflow Climate Sensitivity under RCP 4.5: a) Between Q_5 and P_{mean} b) Between Q_{95} and P_{mean}; Streamflow Climate Sensitivity under RCP 8.5: c) Between Q_5 and P_{mean} d) Between Q_{95} and P_{mean}

Streamflow climate sensitivity is a comparison between change in precipitation to the change in streamflow values. Figure 4-6 indicates the percentage changes in High flows (Q_5) and Low flows (Q_{95}) against the percentage changes in (P_{mean}) for both RCP 4.5 and RCP 8.5 scenarios for the end century period (2071-2100). These percentage changes are calculated relative to the baseline period (1974-2003) values of Q_5, Q_{95} and P_{mean}. It is evident from the figure that the streamflow is highly sensitive to the precipitation and holds a somewhat linear relation. For the watershed under consideration, the streamflow climate sensitivity can be considered high. In other words, a small shift in the precipitation regime will cause an enormous shift in the streamflow regime. The low flows in particular, are extremely sensitive to the precipitation changes. For instance, an average 20% increase in annual precipitation causes up to an average 150% increase in annual low flows (Q_{95}) while an average 25% increase in annual precipitation cause an average of 80% increase in the annual high flows (Q_5).

4.4.3 Analysis of flow duration curves (FDC)

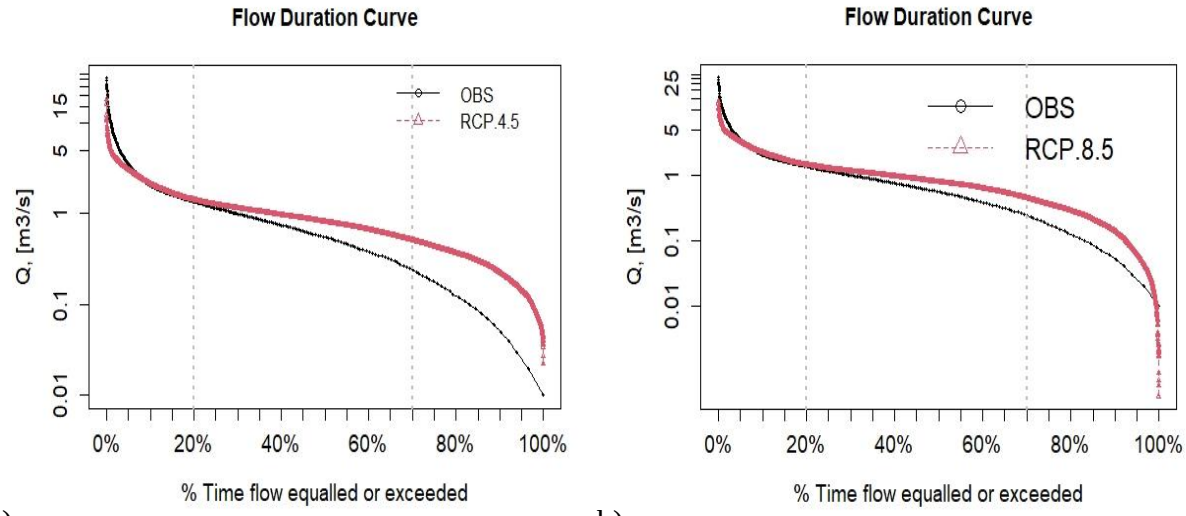

a) b)

Figure 4-7: Flow Duration Curves (FDC) for observed and end century projections under a) RCP 4.5 and b) RCP 8.5 scenarios

Flow duration curves (FDC) for the GALR4950 outlet of LREW are plotted for comparing the exceedance probability of streamflow, between the base period (1974-2003) and the end-century period (2071-2100) to infer the change in streamflow patterns in the end-century period. Figure 4-7 depicts the FDC for RCP 4.5 and RCP 8.5 for baseline observed (1974-2003) and end-century periods (2071-2100) for the study area. The projected FDC values predict a slight decrease in high flows, but an increase in medium and low flows during the end century period. The increase in low flows is comparatively higher than medium flows. Increase in low flows (flow exceedance > 70%) indicate the decrease in drought events in the end century period when compared to the baseline period. The slight decrease in the high flows (flow exceedance < 20%) indicates the reduced susceptibility of the flooding in the study area for the end century period in comparison to the baseline period. The flow duration curve flattens during Q20-Q70 (medium flows), which usually indicates an increase in the contribution of groundwater towards the river flow which is instrumental in sustaining the flow throughout the year. Some unpredictable factors like change in LULC and/or unprecedented extreme climatic events can influence these inferences.

4.4.4 Water budget analysis

Water budget analysis can be considered as a tool to help the modeller understand different hydrological processes and the water cycle components like evapotranspiration, total water yield and surface runoff occurring within the watershed. The average annual, monthly and seasonal water budget breakdowns for end-century period (2071-2100) are given below.

4.4.4.1 Average annual water budget

Average annual precipitation for the study area for end century period was 1251 mm, out of which approximately 22%, i.e., 273 mm was lost as evapotranspiration. The remaining 75% constituted the total water yield (946 mm) out of which 326 mm was attributed to surface runoff and 574 mm was attributed to groundwater. Lower rates of evaporation can be attributed to quick percolation of water into the soils. The study area is predominantly sandy loam with high infiltration rate of about 5 cm/hr (Choudhary and Athira, 2021).

Table 4-3 presents the average annual water budget for 2071-2100 is presented. In accordance with prior research, streamflow generation ranges up to about 30% of the yearly precipitation (Rajat and Athira, 2021).

Table 4-3: Average annual water budget

Precipitation (mm)	1251
Evapotranspiration(mm)	273
Total water yield (mm)	946
Surface runoff (mm)	326
Groundwater (mm)	574

4.4.4.2 Average monthly water budget

The average monthly water budget analysis is presented in Table 4-4 and shows the variations in the hydrological components throughout the year. It is evident that the surface runoff is lowest is summer (July) due to relatively high values of evapotranspiration under the peak summer heat. Surface runoff then increases abruptly in August due to increased precipitation.

Evapotranspiration is at its highest during June due to increased solar radiation, hotter temperatures and agricultural growth.

Table 4-4: Average monthly water budget

Month	Precipitation (mm)	Evapotranspiration (mm)	Surface runoff (mm)	Total water yield (mm)	Groundwater (mm)
1	89	4	25	81	76
2	131	6	46	104	67
3	115	8	38	109	71
4	120	14	40	111	59
5	77	54	18	82	62
6	99	81	13	57	34
7	116	54	11	47	27
8	160	19	44	85	34
9	75	13	13	60	40
10	60	8	16	61	40
11	85	6	23	61	40
12	123	5	39	86	55

4.4.4.3 Seasonal water budget

Seasonal water budget analysis was performed to obtain insight into the variation of the hydrological components across seasons. The division of seasons in this case follows: winter (December, January, February, and March), spring (April and May), summer (June, July, August and September) and fall (October and November). Table 4-5 presents the average values of the hydrological components followed by the percentage breakdowns for each. Summer has the maximum evapotranspiration (47% of annual evapotranspiration), while winter months demonstrated the lowest (5% of annual evapotranspiration). The highest surface runoff occurred in winter months (35% of the annual surface runoff) while summer and fall had low runoff values (about 19% of the annual surface runoff).

Table 4-5: Seasonal water budget values

Season	Precipitation (mm) %	Evapotranspiration (mm) %	Surface runoff (mm) %	Total water yield (mm) %	Groundwater (mm) %
Winter	115 (29)	6 (6)	37 (35)	95 (30)	67 (33)
Spring	98 (25)	34 (39)	29 (27)	97 (31)	60 (30)
Summer	112 (28)	42 (47)	20 (19)	62 (20)	34 (17)
Fall	73 (18)	7 (8)	20 (19)	61 (19)	40 (20)

4.5 Uncertainty decomposition

This subsection presents the breakdown of uncertainty as percentage of variance. The uncertainty decomposition is presented as overall variance as well as monthly variance breakdown for mean flow, low flow and high flow.

4.5.1 Overall variance

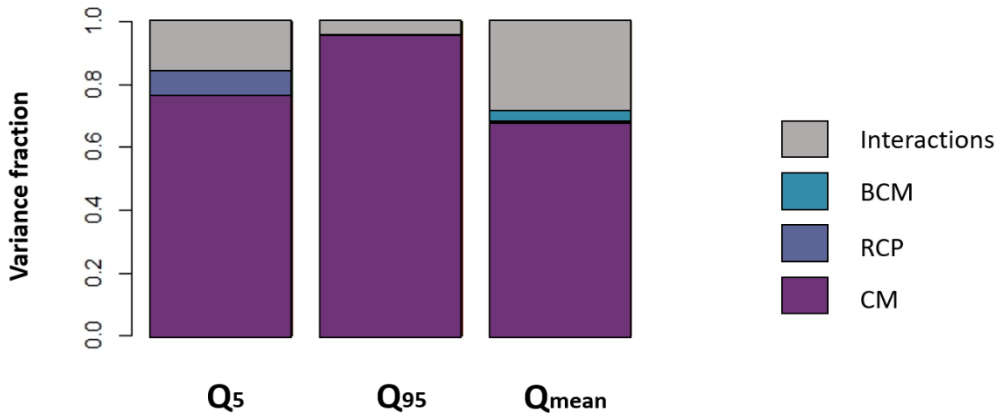

Figure 4-8: Overall uncertainty decomposition for Q_{mean}, Q_5 and Q_{95} for the end century (2071-2100) period

The results in Figure 4-8 show that the Climate Model (CM) uncertainty is the biggest contributor toward the total uncertainty. The sum total of all the interaction uncertainties (CM:RCP + CM:BCM + BCM:RCP + CM:BCM:RCP) almost always have a higher mean relative contribution than the other uncertainty components (namely RCP and BCM), but in all cases, much lower than that of CM uncertainty. The relative contribution of BCM is negligible in case of extreme flows but visibly significant in case of mean flow.

4.5.2 Monthly variance

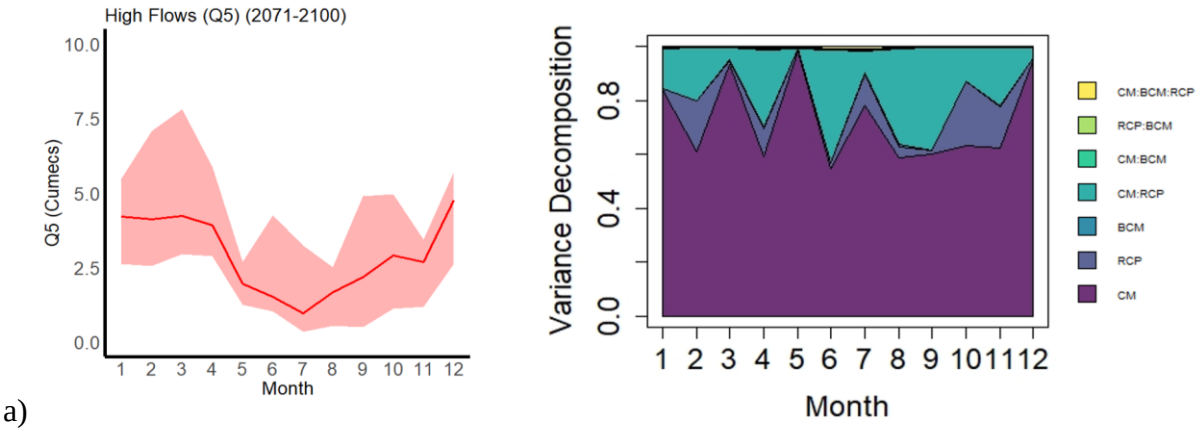

a)

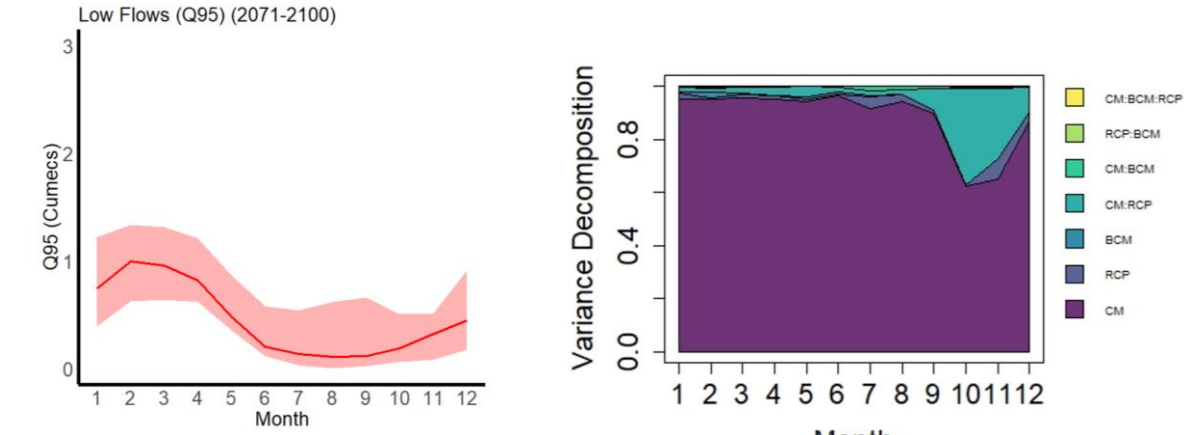

b)

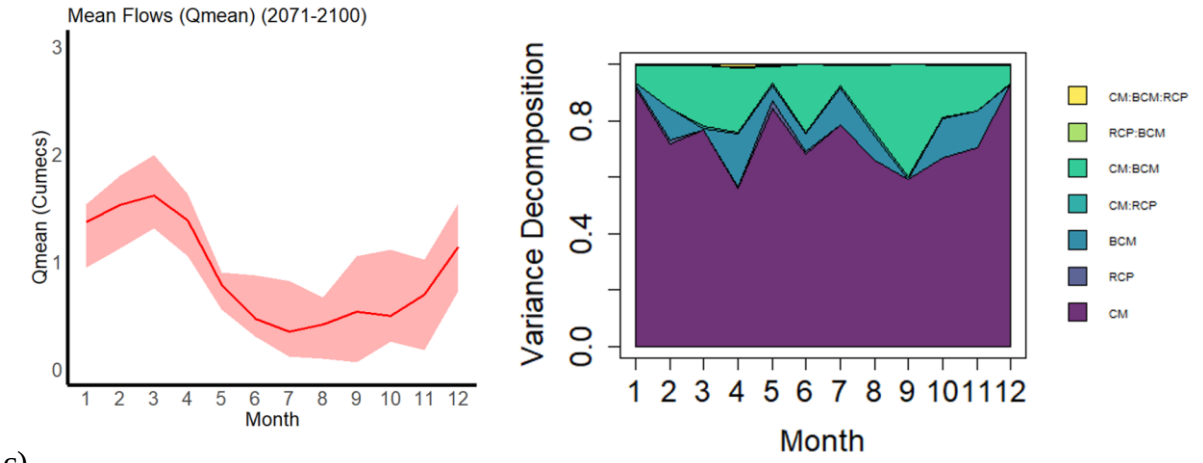

c)

Figure 4-9: Month-wise Variance Decomposition of a) Q_5, b) Q_{95} and c) Q_{mean} for the end century period (2071-2100)

From Figure 4-9, it is evident that in case of High flows (Q_5), there is a wide range of fluctuation for the CM uncertainty. CM being the biggest uncertainty contributor varies from 55% in June to around 98% in May. The interaction between CM and RCP is the second biggest contributor followed by RCP scenario. All the other factors and their interactions are insignificant in comparison to the total uncertainty. For Low flows (Q_{95}), the uncertainty contribution of CM remains relatively constant, except for the dry season, where the interaction between CM and RCP becomes significant. CM remains the largest uncertainty contributor varying from around 50% in October to 95% in June. RCP scenario also notably contributes to the total uncertainty in this case. In case of Mean Flow (Q_{mean}) however, the interaction between CM and BCM is one of the predominant uncertainty contributors. The choice of BCM also strongly affects the total uncertainty. CM is still the largest contributor toward total uncertainty ranging between approximately 55% in April to 90% in January. The proportional contribution of Climate Model (CM) uncertainty for high flow (Q_5) is typically consistent with that for mean flow for the future period (end-century), especially during the dry season. CM is the most important source of uncertainty in the end-century projections.

4.5.3 Interaction plots for uncertainty decomposition of Q_{mean}

Interaction effect between the factors correspond to the combined effects of the considered factors (CM, BCM and RCP) on the dependent measure. One of the major advantages of ANOVA apart from being easy to apply is its capability to consider and assess interaction effects. In this study, a 3-way ANOVA was performed and Figure 4-10 interactions that help us in understanding the combined effect of factor interactions for every month of the year for Q_{mean} for 2071-2100.

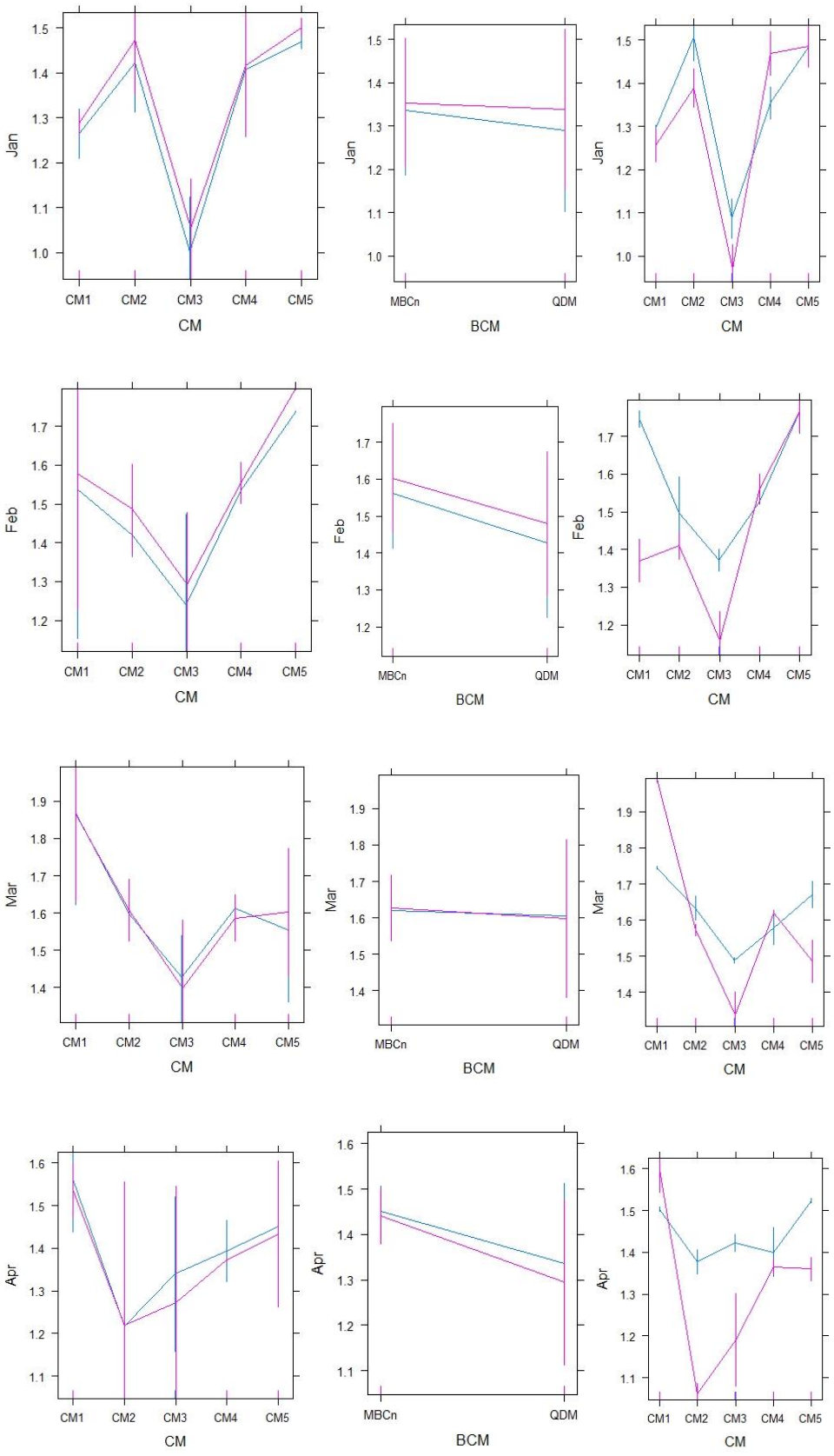
Jan
Feb
Mar
Apr
CM1
CM2
CM3
CM4
CM5
CM
MBCn
QDM
BCM

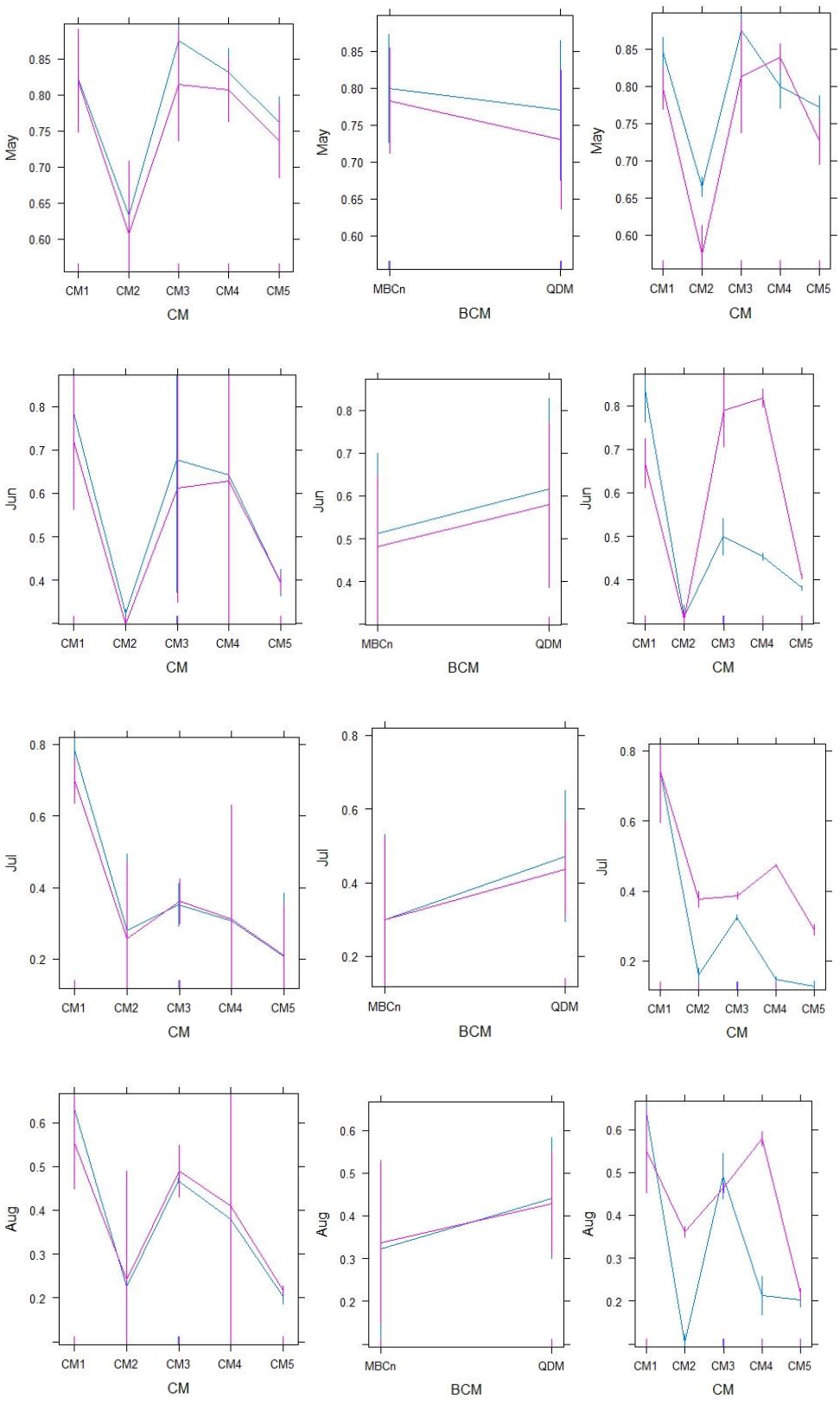
May
0.85
0.80
0.75
0.70
0.65
0.60
CM1 CM2 CM3 CM4 CM5
CM
May
0.85
0.80
0.75
0.70
0.65
0.60
MBCn QDM
BCM
May
0.85
0.80
0.75
0.70
0.65
0.60
CM1 CM2 CM3 CM4 CM5
CM
Jun
0.8
0.7
0.6
0.5
0.4
CM1 CM2 CM3 CM4 CM5
CM
Jun
0.8
0.7
0.6
0.5
0.4
MBCn QDM
BCM
Jun
0.8
0.7
0.6
0.5
0.4
CM1 CM2 CM3 CM4 CM5
CM
Jul
0.8
0.6
0.4
0.2
CM1 CM2 CM3 CM4 CM5
CM
Jul
0.8
0.6
0.4
0.2
MBCn QDM
BCM
Jul
0.8
0.6
0.4
0.2
CM1 CM2 CM3 CM4 CM5
CM
Aug
0.6
0.5
0.4
0.3
0.2
CM1 CM2 CM3 CM4 CM5
CM
Aug
0.6
0.5
0.4
0.3
0.2
MBCn QDM
BCM
Aug
0.6
0.5
0.4
0.3
0.2
CM1 CM2 CM3 CM4 CM5
CM

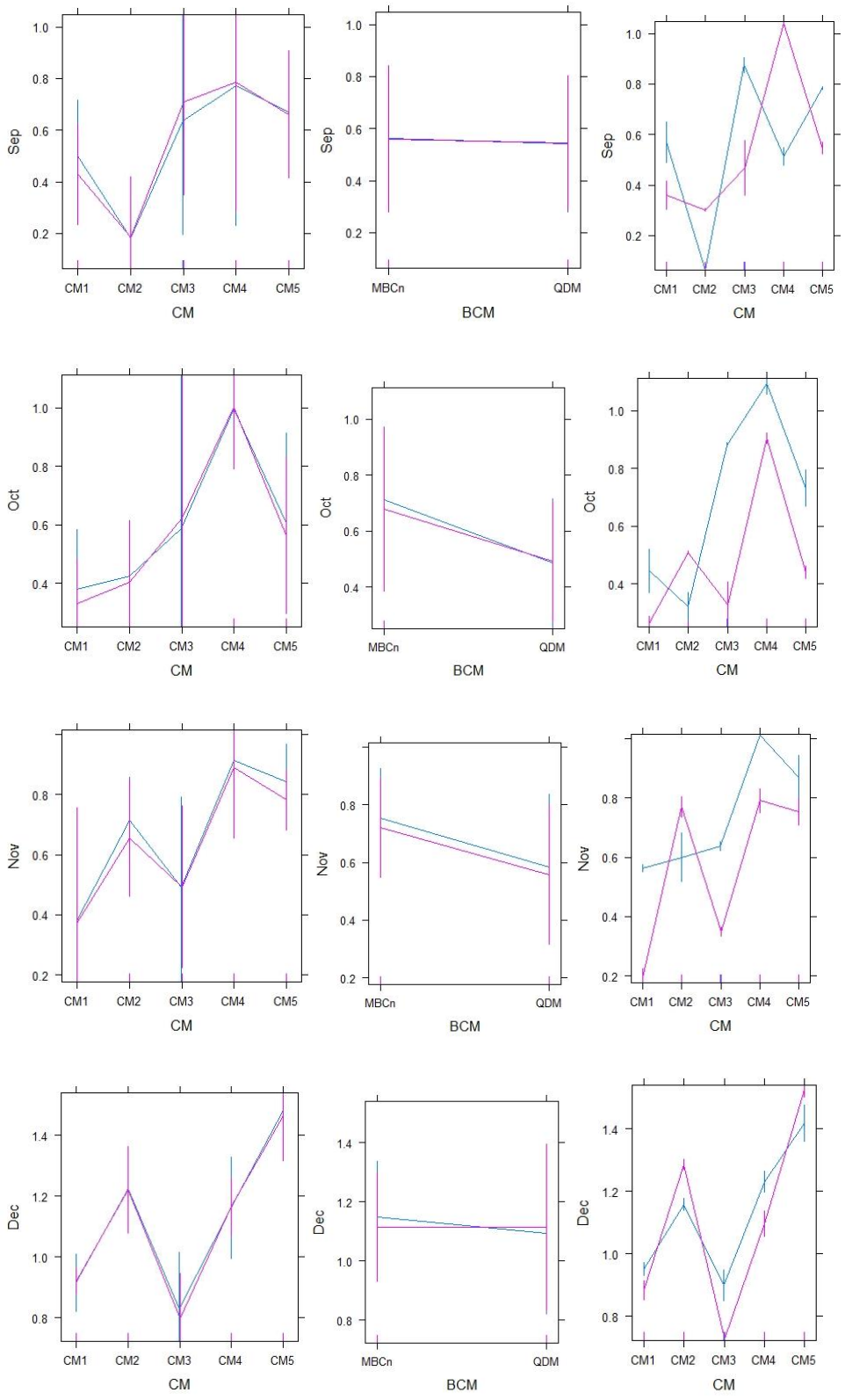

Figure 4-10: Interaction plots for each month corresponding to (CM: RCP), (BCM: RCP) and (CM: BCM) from left to right

From Figure 4-10, multiple types of interactions are observed as follows. The interaction cases where the lines do not meet are called “ordinal interactions”. In such cases, if the two lines are almost parallel, it indicates that there is no significant interaction effect between the considered factors. If the lines are not touching, but still significantly skewed, then there is a chance of interaction effects being prevalent, given enough statistical power. In the case of plots with lines crossing each other, they indicate “disordinal interactions” (Stevens et al., 2016). These interactions are hard to infer. In the case of disordinal interactions with heavy irregularities, the respective main interaction effects should not be inferred. An f-test should be performed to directly ascertain if the main factors are effective towards total variance.

In this study, the interactions between BCM and RCP and the interactions between CM and RCP are mostly ordinal and they can be safely read to infer the extent of influence the interactions contribute while the interactions between CM and BCM are highly disordinal. In this case a separate f-test can be run to check if the main factors CM and BCM and their interactions CM: BCM hold significant contribution towards the total variance of the modelled metric (Q_{mean} in this case).

CHAPTER 5: CONCLUSIONS

This study evaluates the overall uncertainty and uncertainty contributions from three sources in the quantification of hydrological impacts of climate change based on the ANOVA method. For this extent, a semi-distributed, physically based hydrological model (SWAT) was used to simulate the 50 sq.km head catchment of the Little River Experimental Watershed (LREW) located in Georgia, USA. Choice of Climate Model projections (CM), Bias Correction methods (BCM) and Representative Concentration Pathway scenarios (RCP) are chosen as factors to investigate their contribution towards the total uncertainty in the modelling process. In order to further investigate the impacts of the factors and their interactions on the streamflow, the flow was expressed in three different metrics namely high flows(Q5), low flows (Q95) and mean flows (Qmean). The main conclusions are as follows.

1. The contributions of the main factors toward the total uncertainty are most significant in case of extreme indicators (Low flow and peak flow) when compared to the mean flow wherein the uncertainties arising out of interactions between the factors account for a significant (>25%) portion of the total uncertainty.

2. For the changes in low, high and mean flows, the choice of Climate Models (CM) remains the leading source of uncertainty. Therefore, considering the influences of CM should be a prerequisite while evaluating climate change impacts on mean, low and high flows.

3. Unlike low and high flows, the choice of Bias Correction Method (BCM) is a major contributor toward uncertainty for the mean flows. Hence, special consideration should be given to BCM and its interacting components in this case.

Regardless of the streamflow metric chosen, CM remained the biggest contributor to total uncertainty in the Climate Change Impact Assessment process. This shows that any positive technological advancement in the field of climate modelling has a scope to greatly decrease the total uncertainty.

ANOVA framework has its own disadvantages like the assumption that the simulated data points are truly gaussian-like i.e., the test is not truly representative if there are outliers present. Additionally, the uncertainty contribution of the interaction between factors is oftentimes difficult to clearly infer (Kim et al., 2019). In this particular study, four out of 5 climate models had the same driving GCM while having a different RCM. This limitedness in true GCM variability is also a limitation, in the sense that true state of the climate variability might not have been represented strictly.

From the prior literature, it is evident that ANOVA was used mainly to decompose uncertainty in climate change impacts measured through simple streamflow metrics like Q_{mean}, Q_{median} and other straightforward output variables. Although these streamflow variables like mean flow confirm the model ability to reproduce runoff volume (Todorovic et al., 2019), they are not truly representative of the catchment response under varied flow segments. To address this issue, hydrologic signatures which are the features of a catchment's hydrologic reaction (Sawicz et al., 2011) are used. Flow duration curves (FDC) and their derivative streamflow metrics can be used for diagnostic evaluation of model and can be truly representative of the catchment under consideration. For a storm event, the FDC_{high} and FDC_{low} are used to understand the catchment response, driven by quick (direct runoff) and slow (groundwater discharge) streamflow generation processes respectively. Also, slope of FDC mid-segment can be used as a streamflow diagnostic

metric. A high slope value indicates a variable flow regime, while a low slope value means a more damped response.

Apart from diagnostic evaluation of the model (Yilmaz et al., 2008; Westerberg et al., 2011; Andréassian et al., 2012; Chilkoti et al. 2019), FDC and their derivative metrics were also employed for grouping catchments (Carrillo et al. 2011; Sawicz et al. 2011). In this regard, the LREW study area considered for this study is deemed to be a "keystone" for understanding coastal plain watersheds (Bosch et al., 2021) and hence, the use of diagnostic and superior representative hydrological signatures which capture the hydrological response of the catchment will give us better insight into climate change impacts measured through the said signatures for a coastal plain watershed in the USA.

There are a lot of sources of uncertainty and hence a wider umbrella study encompassing an n-way ANOVA including not only BCM, CM, RCP but also other factors like hydrological model choice, precipitation datasets, hydrological parameters, internal variability, etc. and their effect on the total uncertainty should be investigated.

Finally, an integrated modelling system which encompasses various phases/methodologies also covering the model structure uncertainties, input uncertainties etc. which is a bundled framework and can be transferable from one variable to another (for instance, the same methodology or system should be effective in uncertainty decomposition of factors for one variable like any streamflow metric should be transferable to another variable like ground flow, ET, etc.) should be the focus of future research.

REFERENCES

Abbaspour, K.C. (2008). "SWAT-CUP2: SWAT Calibration and Uncertainty Programs A User Manual." Eawag, Duebendorf, Switzerland.

Abbaspour, K.C., Yang, J., Maximov, I., Siber, R., Bogner, K., Mieleitner, J., Zobrist, J. and Srinivasan, R. (2007). "Spatially distributed modelling of hydrology and water quality in the pre-alpine/alpine Thur watershed using SWAT." Journal of Hydrology, 333(2-4), 413–430.

Abbaspour, K.C., Johnson, C.A. and van Genuchten, M.T. (2004). "Estimating uncertain flow and transport parameters using a sequential uncertainty fitting procedure." Vadose Zone Journal, 3(4), 1340–1352.

Abbaspour, K. C., Rouholahnejad, E., Vaghefi, S., Srinivasan, R., Yang, H., and Kløve, B. (2015). "A continental-scale hydrology and water quality model for Europe: Calibration and uncertainty of a high-resolution large-scale SWAT model." Journal of Hydrology, 524, 733–752.

Addor, Nans & Rössler, Ole & Bosshard, Nina & Huss, Matthias & Weingartner, Rolf & Seibert, Jan. (2014). Robust changes and sources of uncertainty in the projected hydrological regimes of Swiss catchments. Water Resources Research. 10.1002/2014WR015549.

Alok K. Sahoo, Paul R. Houser, Craig Ferguson, Eric F. Wood, Paul A. Dirmeyer, Menas Kafatos, Evaluation of AMSR-E soil moisture results using the in-situ data over the Little River Experimental Watershed, Georgia, Remote Sensing of Environment, Volume 112, Issue 6, 2008, Pages 3142-3152, ISSN 0034-4257, https://doi.org/10.1016/j.rse.2008.03.007.

Arnell, N.W., 2011. Uncertainty in the relationship between climate forcing and hydrological response in UK catchments. Hydrol. Earth Syst. Sci. 15, 897–912. https://doi.org/10.5194/hess15-897-2011

Arnold, J. G., Srinivasan, R., Muttiah, R. S., & Williams, J. R. (1998). Large area hydrologic modeling and assessment part I: model development 1. JAWRA Journal of the American Water Resources Association, 34(1), 73-89.

Aryal, A., Shrestha, S. & Babel, M.S. Quantifying the sources of uncertainty in an ensemble of hydrological climate-impact projections. Theor Appl Climatol **135,** 193–209 (2019). https://doi.org/10.1007/s00704-017-2359-3

Athira, P., Sudheer, K.P., 2015. A method to reduce the computational requirement while assessing uncertainty of complex hydrological models. Stoch. Environ. Res. Risk Assess. 29, 847–859. https://doi.org/10.1007/s00477-014-0958-4

Bates, B.C. and Campbell, E.P. (2001). "A Markov chain Monte Carlo scheme for parameter estimation and inference in conceptual rainfall–runoff modeling." Water Resources Research, 37(4), 937–947.

Bedient, P.B., Huber, W.C., Vieux, B.E., 2008. Hydrology and floodplain analysis.

Beven, K. and Binley, A. (1992). "The future of distributed models – model calibration and uncertainty prediction." Hydrological Processes, 6(3), 279–298.

Beven, K., and Freer, J. (2001). “Equifinality, data assimilation, and uncertainty estimation in mechanistic modelling of complex environmental systems using the GLUE methodology.” Journal of hydrology, 249(1), 11–29.

Beven, K., 2016. Facets of uncertainty: epistemic uncertainty, non-stationarity, likelihood, hypothesis testing, and communication. Hydrol. Sci. J. 61, 1652–1665. https://doi.org/10.1080/02626667.2015.1031761

Bosch, D. D., J. M. Sheridan, H. L. Batten, and J. G. Arnold. 2004. Evaluation of the SWAT model on a coastal plain agricultural watershed. Trans. ASAE 47(5): 1493-1506.

Bosch, David & Sullivan, D.G. & Sheridan, Joseph. (2006). Hydrologic Impacts of Land-Use Changes in Coastal Plain Watersheds. Transactions of the ASABE. 49. 10.13031/2013.20416.

Bosch, D. D., Sheridan, J. M., Lowrance, R. R., Hubbard, R. K., Strickland, T. C., Feyereisen, G. W., and Sullivan, D. G. (2007), Little River Experimental Watershed database, *Water Resour. Res.*, 43, W09470, doi:10.1029/2006WR005844.

Bosch, D. D., Coffin, A. W., Sheridan, J., Pisani, O., Endale, D. M., & Strickland, T. C. (2021). Little River Experimental Watershed, a keystone in understanding of coastal plain watersheds. *Hydrological Processes*, 35(8), e14334. https://doi-org.ledproxy2.uwindsor.ca/10.1002/hyp.14334

Bosshard, T., Carambia, M., Goergen, K., Kotlarski, S., Krahe, P., Zappa, M., and Schär, C. (2013), Quantifying uncertainty sources in an ensemble of hydrological climate-impact projections, Water Resour. Res., 49, 1523– 1536, doi:10.1029/2011WR011533.

Cannon, A.J. Multivariate quantile mapping bias correction: an *N*-dimensional probability density function transform for climate model simulations of multiple variables. Clim Dyn **50,** 31–49 (2018). https://doi-org.ledproxy2.uwindsor.ca/10.1007/s00382-017-3580-6

Cannon AJ, Sobie SR, Murdock TQ (2015) Bias correction of simulated precipitation by quantile mapping: how well do methods preserve relative changes in quantiles and extremes? J Clim 28(17):6938–6959. doi:10.1175/JCLI-D-14-00754.1

Chegwidden, O.S., Nijssen, B., Rupp, D.E., Arnold, J.R., Clark, M.P., Hamman, J.J., Kao, S.-C., Mao, Y., Mizukami, N., Mote, P. W., Pan, M., Pytlak, E. and Xiao, M. (2019) How do modeling decisions affect the spread among hydrologic climate change projections? Exploring a large ensemble of simulations across a diversity of hydroclimates. Earth's Future, 7, 623–637.

Chen, Jiahua & Eeden, Constance & Zidek, James. (2010). Uncertainty and the conditional variance. Statistics & Probability Letters. 80. 1764-1770. 10.1016/j.spl.2010.07.021.

Chilkoti, Vinod, "Impacts of climate change on hydropower generation and developing adaptation measures through hydrologic modeling and multi-objective optimization" (2019). *Electronic Theses and Dissertations*. 7691. https://scholar.uwindsor.ca/etd/7691

Cho, J., Lowrance, R.R., Bosch, D.D., Strickland, T.C., Her, Y. and Vellidis, G. (2010), Effect of Watershed Subdivision and Filter Width on SWAT Simulation of a Coastal Plain Watershed. JAWRA Journal of the American Water Resources Association, 46: 586-602. https://doi-org.ledproxy2.uwindsor.ca/10.1111/j.1752-1688.2010.00436.x

Cho, J., Bosch, D., Vellidis, G., Lowrance, R. and Strickland, T. (2013), Multi-site evaluation of hydrology component of SWAT in the coastal plain of southwest Georgia. Hydrol. Process., 27: 1691-1700. https://doi-org.ledproxy2.uwindsor.ca/10.1002/hyp.9341

Choudhary, R., Athira, P. Effect of root zone soil moisture on the SWAT model simulation of surface and subsurface hydrological fluxes. *Environ Earth Sci* **80,** 620 (2021). https://doi.org/10.1007/s12665-021-09912-z

Datta, A. R. and Bolisetti, T. (2013), Application of variance decomposition approach in the uncertainty analysis of a hydrological model. *Canadian Journal of Civil Engineering*. **40**(4): 373-381. https://doi.org/10.1139/cjce-2012-0337

Datta, Arpana Rani, "Evaluation of Implicit and Explicit Methods of Uncertainty Analysis on a Hydrological Modeling" (2011). *Electronic Theses and Dissertations*. 5397. https://scholar.uwindsor.ca/etd/5397

David D. Bosch, Clint C. Truman, Thomas L. Potter, Larry T. West, Timothy C. Strickland, Robert K. Hubbard, Tillage and slope position impact on field-scale hydrologic processes in the South Atlantic Coastal Plain, Agricultural Water Management, Volume 111, 2012, Pages 40-52, ISSN 0378-3774, https://doi.org/10.1016/j.agwat.2012.05.002.

David D. Bosch, Jeff G. Arnold, Peter G. Allen, Kyoung-Jae Lim, Youn Shik Park, Temporal variations in baseflow for the Little River experimental watershed in South Georgia, USA, Journal of Hydrology: Regional Studies, Volume 10, 2017, Pages 110-121, ISSN 2214-5818, https://doi.org/10.1016/j.ejrh.2017.02.002.

Deser C, Phillips AS, Alexander MA (2010) Twentieth century tropical sea surface temperature trends revisited. Geophys Res Lett 37:L10701. doi:10.1029/2010GL043321

Deser, C., Phillips, A., Bourdette, V., and Teng, H. (2012). "Uncertainty in climate change projections: the role of internal variability." Climate Dynamics, 38(3–4), 527–546.

Dobler, C., Hagemann, S., Wilby, R. L., and Stötter, J. (2012). “Quantifying different sources of uncertainty in hydrological projections in an Alpine watershed.” Hydrology and Earth System Sciences, 16(11), 4343–4360.

Donnelly, C., Greuell, W., Andersson, J., Gerten, D., Pisacane, G., Roudier, P., Ludwig, F., 2017. Impacts of climate change on European hydrology at 1.5, 2 and 3 degrees mean global warming above preindustrial level. Climatic Change 143, 13–26. https://doi.org/10.1007/s10584-017-1971-7

Duan, Q., Sorooshian, S. and Ibbitt, R. (1988). "A maximum likelihood criterion for use with data collected at unequal time intervals." Water Resources Research, 24(7), 11631173.

Eckhardt, K., Haverkamp, S., Fohrer, N., Frede, H.-G., 2002b. SWAT-G, a version of SWAT99.2 modified for application to low mountain range catchments. Physics and Chemistry of the Earth, in press.

Engeland, K., Renard, B., Steinsland, I. and Kolberg, S. (2010). "Evaluation of statistical models for forecast errors from the HBV model." Journal of Hydrology, 384(1-2), 142155.

Feyereisen, G. W., Lowrance, R., Strickland, T. C., Sheridan, J. M., Hubbard, R. K., and Bosch, D. D. (2007), Long-term water chemistry database, Little River Experimental Watershed, southeast Coastal Plain, United States, *Water Resour. Res.*, 43, W09474, doi:10.1029/2006WR005835.

Giuntoli, I., Villarini, G., Prudhomme, C. *et al.* Uncertainties in projected runoff over the conterminous United States. *Climatic Change* **150,** 149–162 (2018). https://doi-org.ledproxy2.uwindsor.ca/10.1007/s10584-018-2280-5

Haile, G. G., Tang, Q., Hosseini Moghari, S.M., Liu, X., Gebremicael, T. G., Leng, G., et al. (2020). Projected impacts of climate change on drought patterns over East Africa. Earth's Future, 8, e2020EF001502. https://doi. org/10.1029/2020EF001502

Her, Y., Yoo, SH., Cho, J. *et al.* Uncertainty in hydrological analysis of climate change: multi-parameter vs. multi-GCM ensemble predictions. *Sci Rep* **9,** 4974 (2019). https://doi-org.ledproxy2.uwindsor.ca/10.1038/s41598-019-41334-7

Hoghooghi, N., Bosch, D.D. and Bledsoe, B.P. (2021), Assessing hydrologic and water quality effects of land use conversion to *Brassica carinata* as a winter biofuel crop in the southeastern coastal plain of Georgia, USA using the SWAT model. GCB Bioenergy, 13: 473-492. https://doi-org.ledproxy2.uwindsor.ca/10.1111/gcbb.12792

Houshmand Kouchi, Delaram & Esmaili, Kazem & Farid, Alireza & Sanaienejad, Seyed & Khalili, Davar & Mikayilov, Fariz. (2017). Sensitivity of Calibrated Parameters and Water Resource Estimates on Different Objective Functions and Optimization Algorithms. Water. 9. 384. 10.3390/w9060384.

IPCC, 2001: Climate Change 2001: The Scientific Basis. Contribution of Working Group I to the Third Assessment Report of the Intergovernmental Panel on Climate Change [Houghton, J.T., Y. Ding, D.J. Griggs, M. Noguer, P.J. van der Linden, X. Dai, K. Maskell, and C.A. Johnson (eds.)]. Cambridge University Press, Cambridge, United Kingdom and New York, NY, USA, 881pp.

J. G. Arnold, D. N. Moriasi, P. W. Gassman, K. C. Abbaspour, M. J. White, R. Srinivasan, C. Santhi, R. D. Harmel, A. van Griensven, M. W. Van Liew, N. Kannan, M. K. Jha (2012). SWAT: Model use, Calibration, and Validation. Transactions of the ASABE. 55(4): 1491-1508. (doi: 10.13031/2013.42256)

Jie Chen, François P. Brissette, Robert Leconte, Uncertainty of downscaling method in quantifying the impact of climate change on hydrology, Journal of Hydrology, Volume 401, Issues 3–4, 2011, Pages 190-202, ISSN 0022-1694, https://doi.org/10.1016/j.jhydrol.2011.02.020.

Karlsson, I.B., Sonnenborg, T.O., Refsgaard, J.C., Trolle, D., Børgesen, C.D., Olesen, J.E., Jeppesen, E., Jensen, K.H., 2016. Combined effects of climate models, hydrological model structures and land use scenarios on hydrological impacts of climate change. J. Hydrol. 535, 301–317. https://doi.org/10.1016/j.jhydrol.2016.01.069

Kavetski, D., Kuczera, G. and Franks, S.W. (2006a). "Bayesian analysis of input uncertainty in hydrological modeling: 1. Theory." Water Resources Research, 42(3), W03407.

K.C. Abbaspour, E. Rouholahnejad, S. Vaghefi, R. Srinivasan, H. Yang, B. Kløve (2015), A continental-scale hydrology and water quality model for Europe: Calibration and uncertainty of a high-resolution large-scale SWAT model, Journal of Hydrology, Volume 524, 2015, Pages 733-752, ISSN 0022-1694, https://doi.org/10.1016/j.jhydrol.2015.03.027.

Krysanova, V., Hattermann, F. and Wechsung, F. (2005), Development of the ecohydrological model SWIM for regional impact studies and vulnerability assessment. Hydrol. Process., 19: 763-783. https://doi-org.ledproxy2.uwindsor.ca/10.1002/hyp.5619

Kuczera, G. (1983). "Improved parameter inference in catchment models. 1. Evaluating parameter uncertainty." Water Resources Research, 19(5), 1151–1162.

Laloy, E., Fasbender, D. and Bielders, C.L. (2010). "Parameter optimization and uncertainty analysis for plot-scale continuous modeling of runoff using a formal Bayesian approach." Journal of Hydrology, 380(1-2), 82-93.

Lee, J.-K., Kim, Y.-O. and Kim, Y. (2017), A new uncertainty analysis in the climate change impact assessment. Int. J. Climatol., 37: 3837-3846. https://doi-org.ledproxy2.uwindsor.ca/10.1002/joc.4957

Lempert, Robert & Schlesinger, Michael & Bankes, Steven. (1996). When We Don't Know the Costs or the Benefits: Adaptive Strategies for Abating Climate Change. Climatic Change. 33. 10.1007/BF00140248.

Maraun, D. Bias Correcting Climate Change Simulations - a Critical Review. Curr Clim Change Rep **2,** 211–220 (2016). https://doi-org.ledproxy2.uwindsor.ca/10.1007/s40641-016-0050-x

Meresa, H., Tischbein, B. & Mekonnen, T. Climate change impact on extreme precipitation and peak flood magnitude and frequency: observations from CMIP6 and hydrological models. *Nat Hazards* **111,** 2649–2679 (2022). https://doi-org.ledproxy2.uwindsor.ca/10.1007/s11069-021-05152-3

Pfannerstill, Matthias, Bieger, Katrin, Guse, Björn, Bosch, David D., Fohrer, Nicola, and Arnold, Jeffrey G., 2017. How to Constrain Multi-Objective Calibrations of the SWAT Model Using Water Balance Components. *Journal of the American Water Resources Association* (JAWRA) 53(3): 532– 546. DOI: 10.1111/1752-1688.12524

Pisani, Oliva & Bosch, David & Coffin, Alisa & Endale, Dinku & Liebert, Dan & Strickland, Timothy. (2020). Riparian land cover and hydrology influence stream dissolved organic matter composition in an agricultural watershed. Science of The Total Environment. 717. 137165. 10.1016/j.scitotenv.2020.137165.

Rajat and P. Athira. 2021. Calibration of hydrological models considering process interdependence: A case study of SWAT model. Environ. Model. Softw. 144, C (Oct 2021). https://doi-org.ledproxy2.uwindsor.ca/10.1016/j.envsoft.2021.105131

Renard B., Kavetski, D., Kuczera, G., Thyer, M. and Franks, S.W. (2010). "Understanding predictive uncertainty in hydrologic modeling: The challenge of identifying input and structural errors." Water Resources Research, 46, W05521.

Schoups, G. and Vrugt, J. (2010)."A formal likelihood function for parameter and predictive inference of hydrologic models with correlated, heteroscedastic, and non Gaussian errors." Water Resources Research, 46(10), W10531.

Schaefli, B., Talamba, D.B. and Musy, A. (2007). "Quantifying hydrological modeling errors through a mixture of normal distributions." Journal of Hydrology, 332(3-4), 303315.

Sheridan, J. M., and R. K. Hubbard. 1987. Transport of solids in streamflow from Coastal Plain watersheds. J. Environ. Quality 16(2): 131−136.

Sheridan, J. M., W. C. Mills, and L. Hester. 1995. Data management for experimental watersheds. Trans. ASAE 11(2): 249−259.

Shirmohammadi, A., J. M. Sheridan, and L. E. Asmussen. 1986. Hydrology of alluvial stream channels in southern coastal plain watersheds. Trans. ASAE 29(1): 135−142.

Sorooshian, S. and Dracup, J.A. (1980). "Stochastic parameter estimation procedures for hydrologic rainfall–runoff models – correlated and heteroscedastic error cases." Water Resources Research, 16(2), 430–442.

Stojkovic, M., & Simonovic, S. P. (2020). Understanding the uncertainty of the lim river basin response to changing climate. *Journal of Hydrologic Engineering*, *25*(9), 05020023.

Tarek, Mostafa & Brissette, François & Arsenault, Richard. (2021). Uncertainty of gridded precipitation and temperature reference datasets in climate change impact studies. Hydrology and Earth System Sciences. 25. 3331-3350. 10.5194/hess-25-3331-2021

Thober, Stephan & Kumar, Rohini & Wanders, Niko & Marx, Andreas & Pan, Ming & Rakovec, Oldrich & Samaniego, Luis & Sheffield, Justin & Wood, Eric & Zink, Matthias. (2018). Multi-model ensemble projections of European river floods and high flows at 1.5, 2, and 3 degree global warming. Environmental Research Letters. 13. 10.1088/1748-9326/aa9e35.

Thyer, M., Renard, B., Kavetski, D., Kuczera, G., Franks, S.W. and Srikanthan, S. (2009). "Critical evaluation of parameter consistency and predictive uncertainty in hydrological modeling: A case study using Bayesian total error analysis." Water Resources Research, 45, W00B14.

Troin, M., Arsenault, R., Martel, J., & Brissette, F. (2018). Uncertainty of Hydrological Model Components in Climate Change Studies over Two Nordic Quebec Catchments, *Journal of Hydrometeorology*, *19*(1), 27-46. Retrieved Jan 14, 2022, from https://journals-ametsoc-org.ledproxy2.uwindsor.ca/view/journals/hydr/19/1/jhm-d-17-0002_1.xml

Van Griensven, A. and W. Bauwens (2001). Integrating modeling of catchments, Water Science and Technology, 43, 7, 321-328.

Van Liew, Michael & Arnold, Jeff & Bosch, David. (2005). Problems and Potential of Auto-Calibrating a Hydrologic Model. Transactions of the American Society of Agricultural Engineers. 48. 10.13031/2013.18514.

Vetter, T., Reinhardt, J., Flörke, M., van Griensven, A., Hattermann, F., Huang, S., Koch, H., Pechlivanidis, I. G., Plötner, S., Seidou, O., et al.: Evaluation of sources of uncertainty in projected hydrological changes under climate change in 12 large-scale river basins, Climatic Change, 141, 419–433, 2017.

Von Storch, H., and F. Zwiers, 2001: Statistical Analysis in Climate Research. Cambridge University Press, 484 pp.

Vrugt, J.A., ter Braak, C.J.F, Clark, M.P., Hyman, J.M. and Robinson, B.A. (2008). "Treatment of input uncertainty in hydrologic modeling: Doing hydrology backward with Markov chain Monte Carlo simulation." Water Resources Research, 44, W00B09.

Vrugt, J.A., Diks, C.G.H., Bouten, W., Gupta, H.V. and Verstraten, J.M. (2005). "Towards a complete treatment of uncertainty in hydrologic modelling: combining the strengths of global optimization and data assimilation." Water Resources Research, 41(1), W01017.

Vrugt, J.A., Gupta, H.V., Bouten, W. and Sorooshian, S. (2003). "A shuffled complex evolution Metropolis algorithm for optimization and uncertainty assessment of hydrologic model parameters." Water Resources Research, 39(8), 1201.

Wang, H.-M., Chen, J., Xu, C.-Y., Zhang, J., Chen, H. (2020). A framework to quantify the uncertainty contribution of GCMs over multiple sources in hydrological impacts of climate change. *Earth'sFuture*, 8,e2020EF001602. https://doi-org.ledproxy2.uwindsor.ca/10.1029/2020EF001602

Whateley, S., and Brown, C. (2016), Assessing the relative effects of emissions, climate means, and variability on large water supply systems, Geophys. Res. Lett., 43, 11,329– 11,338, doi:10.1002/2016GL070241.

Wilby, R.L., Harris, I., 2006. A framework for assessing uncertainties in climate change impacts: Low-flow scenarios for the River Thames, UK. Water Resour. Res. 42, doi:10.1029/2005WR004065. https://doi.org/10.1029/2005WR004065

Yang, J., Reichert, P., Abbaspour, K.C. and Yang, H. (2007a). "Hydrological modelling of the Chaohe Basin in China: statistical model formulation and Bayesian inference." Journal of Hydrology, 340(3-4), 167–182.

Yang, J., Reichert, P. and Abbaspour, K.C. (2007b). "Bayesian uncertainty analysis in distributed hydrologic modeling: a case study in the Thur River basin (Switzerland)." Water Resources Research, 43(10), W10401.

Yip, S., Ferro, C. A., Stephenson, D. B., and Hawkins, E.: A simple, coherent framework for partitioning uncertainty in climate predictions, J. Climate, 24, 4634–4643, 2011.

Yongdai Kim, Ilsang Ohn, Jae-Kyoung Lee, Young-Oh Kim, Generalizing uncertainty decomposition theory in climate change impact assessments, Journal of Hydrology X, Volume 3, 2019, 100024, ISSN 2589-9155, https://doi.org/10.1016/j.hydroa.2019.100024

Zhang, S., Chen, J., & Gu, L. (2022). Overall uncertainty of climate change impacts on watershed hydrology in China. *International Journal of Climatology*, 42(1), 507– 520. https://doi-org.ledproxy2.uwindsor.ca/10.1002/joc.7257

Zhiying Li, Haiyan Fang, Impacts of climate change on water erosion: A review, Earth-Science Reviews, Volume 163, 2016, Pages 94-117, ISSN 0012-8252, https://doi.org/10.1016/j.earscirev.2016.10.004

APPENDICES

A-1 Trends in temperature timeseries

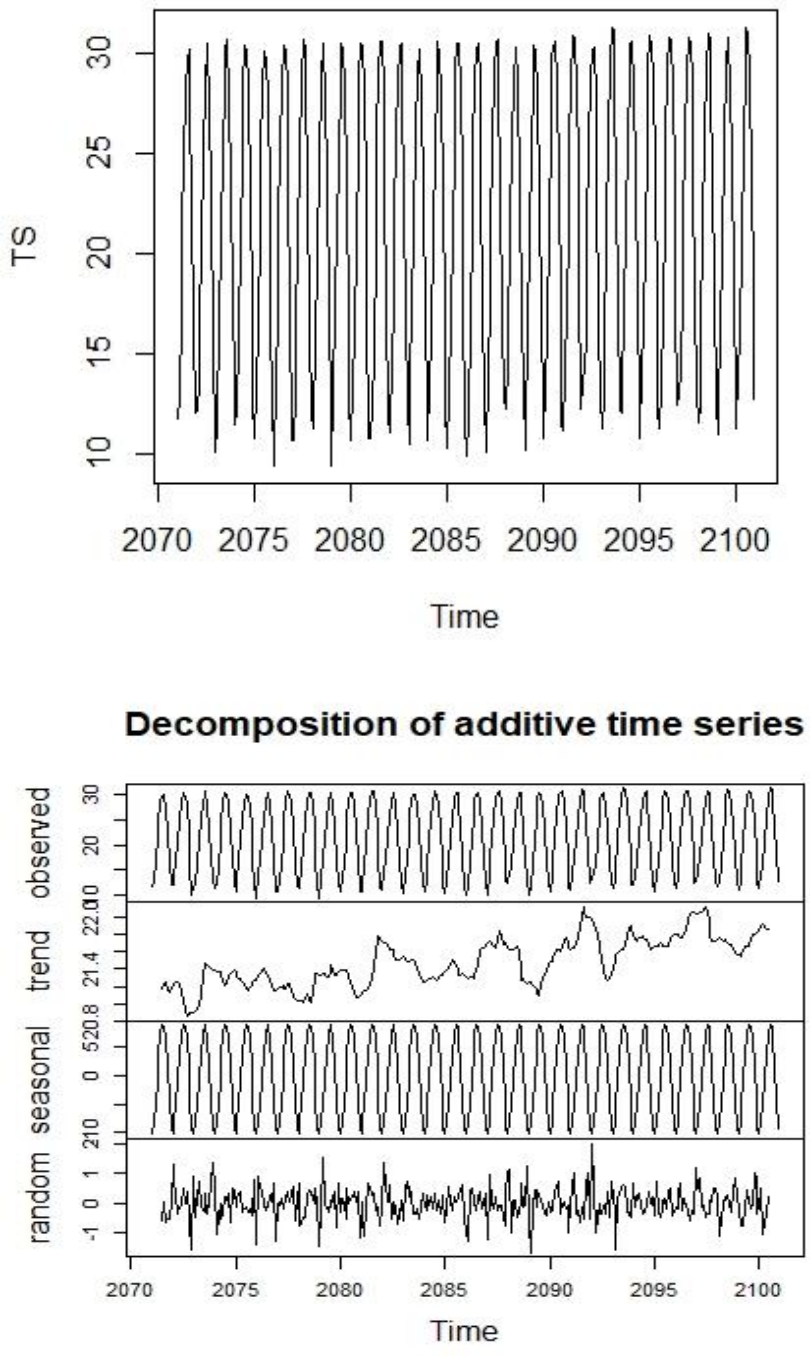

Figure A-1: Trends in mean temperature timeseries (TS) and decomposition for the end century period (2071-2100)

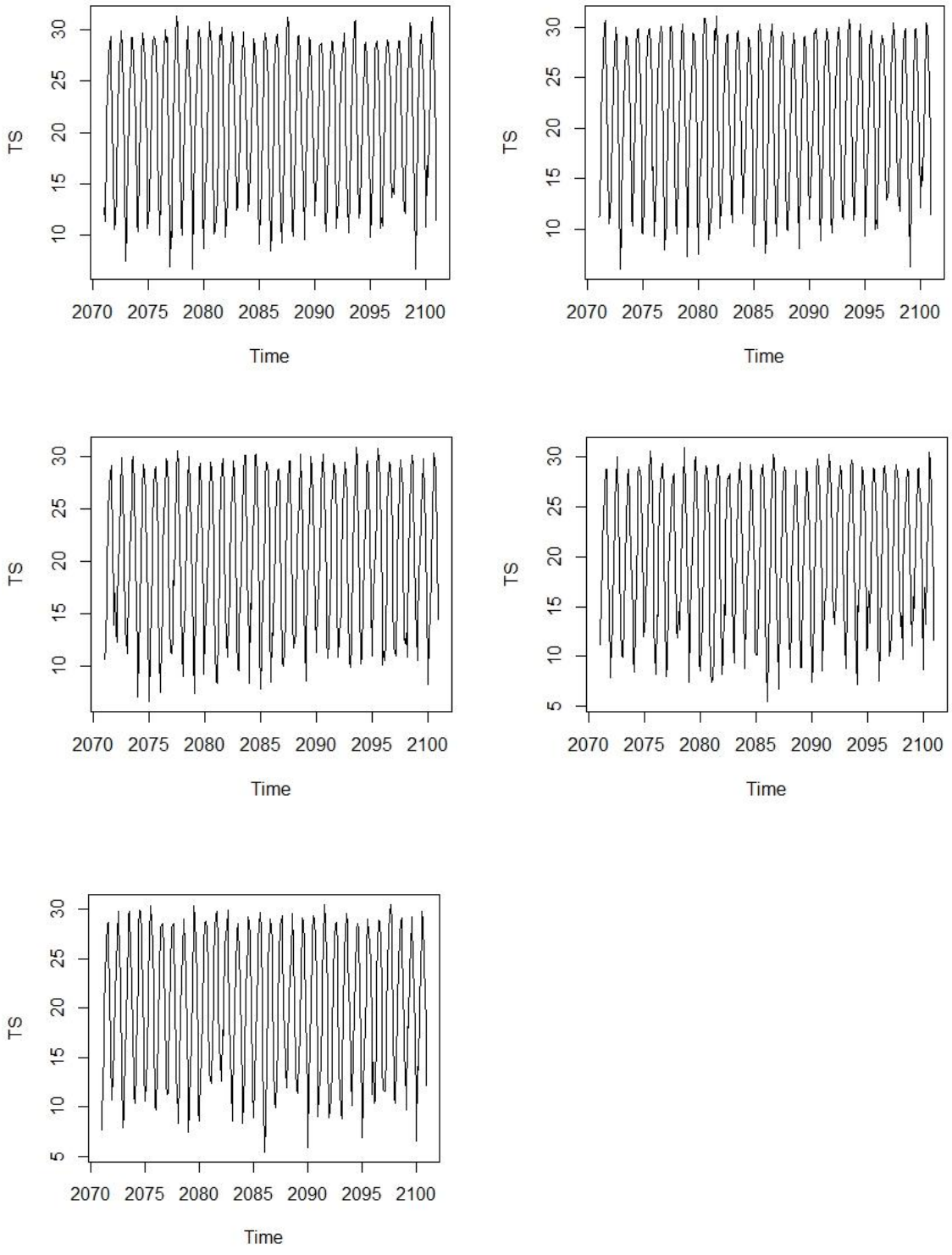

Figure A-2: Temperature trends for 5 CM under QDM bias correction for RCP 4.5 (2071-2100)

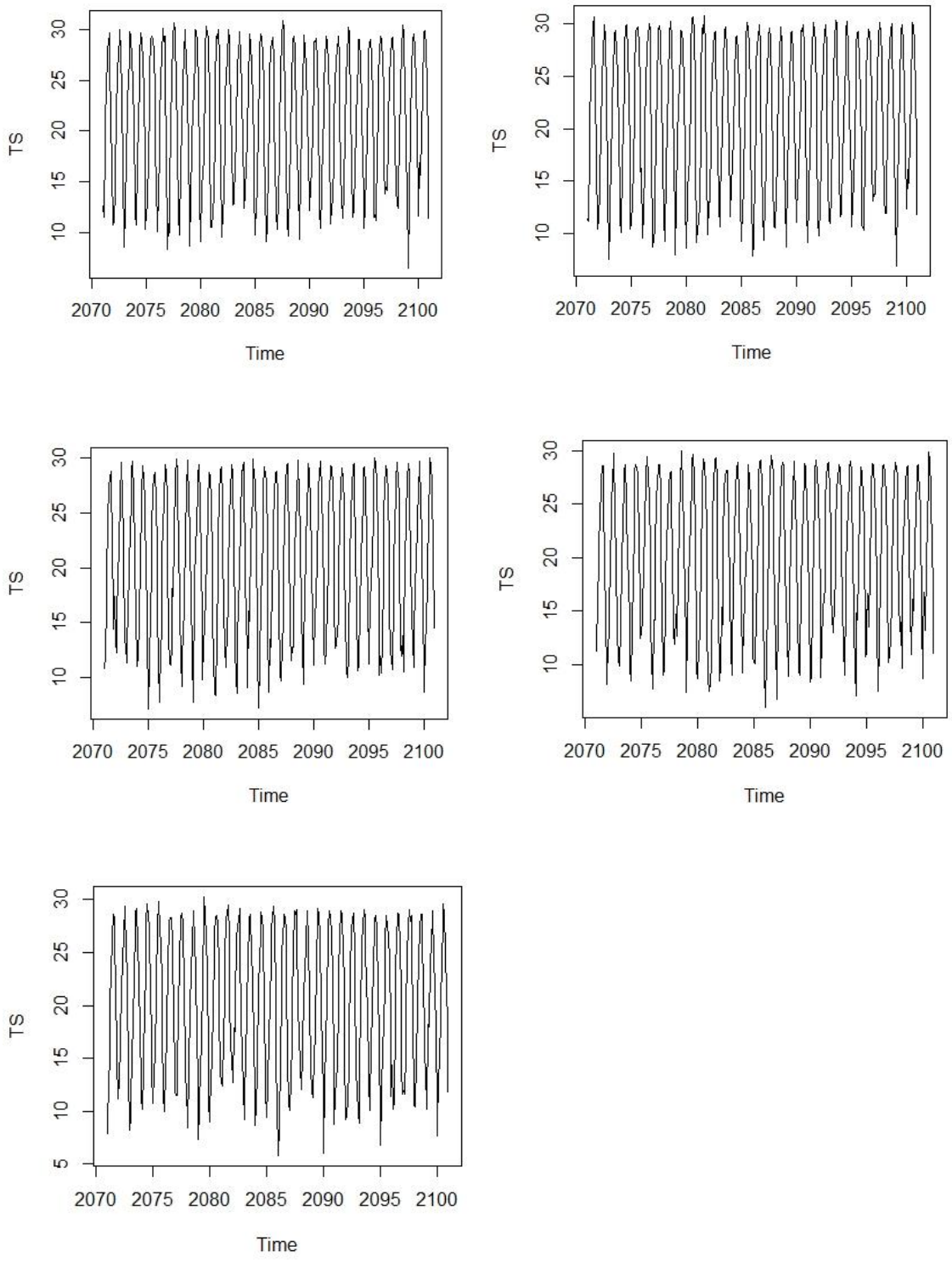

Figure A-3: Temperature trends for 5 CM under MBCn bias correction for RCP 4.5 (2071-2100)

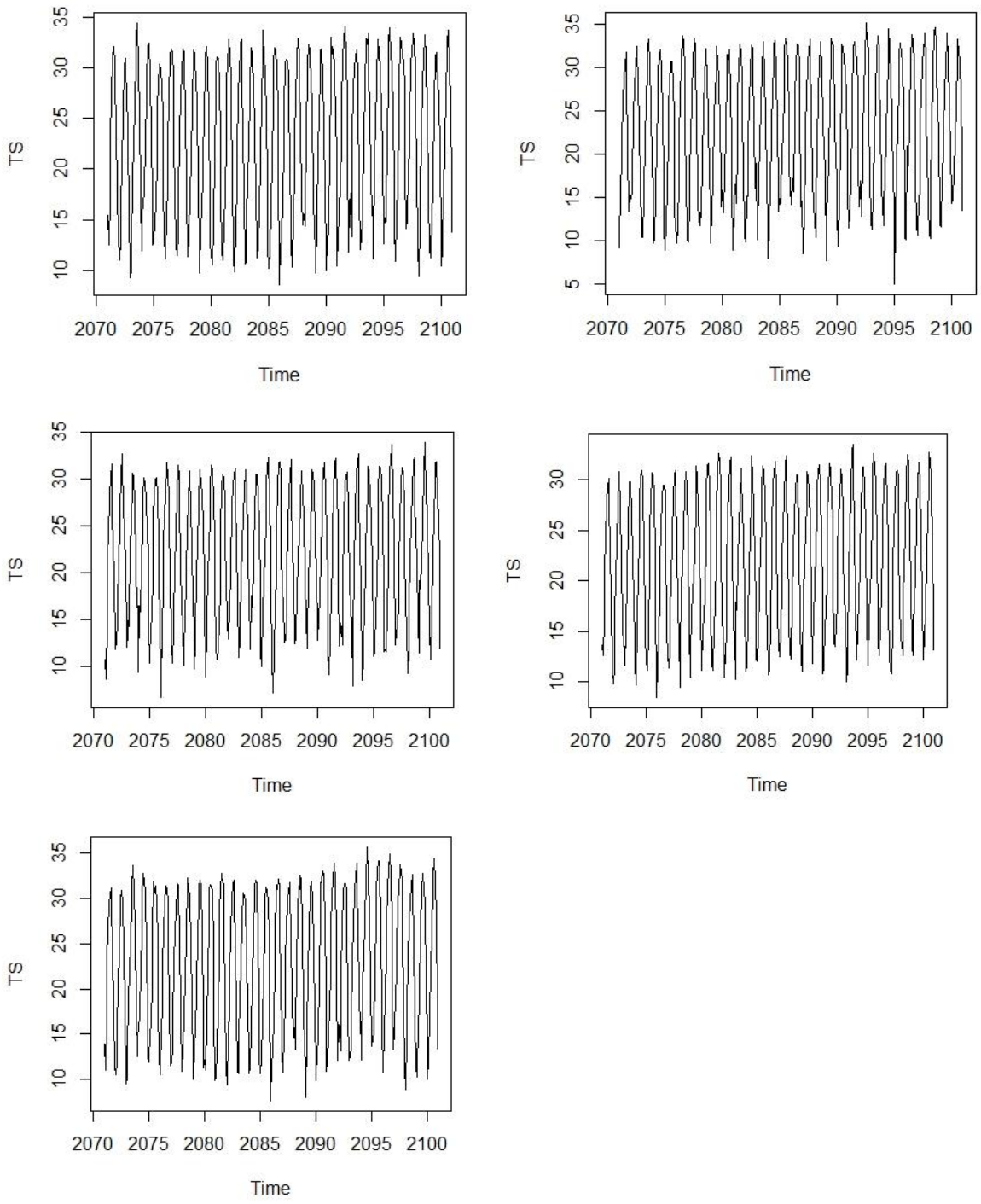

Figure A-4: Temperature trends for 5 CM under QDM bias correction for RCP 8.5 (2071-2100)

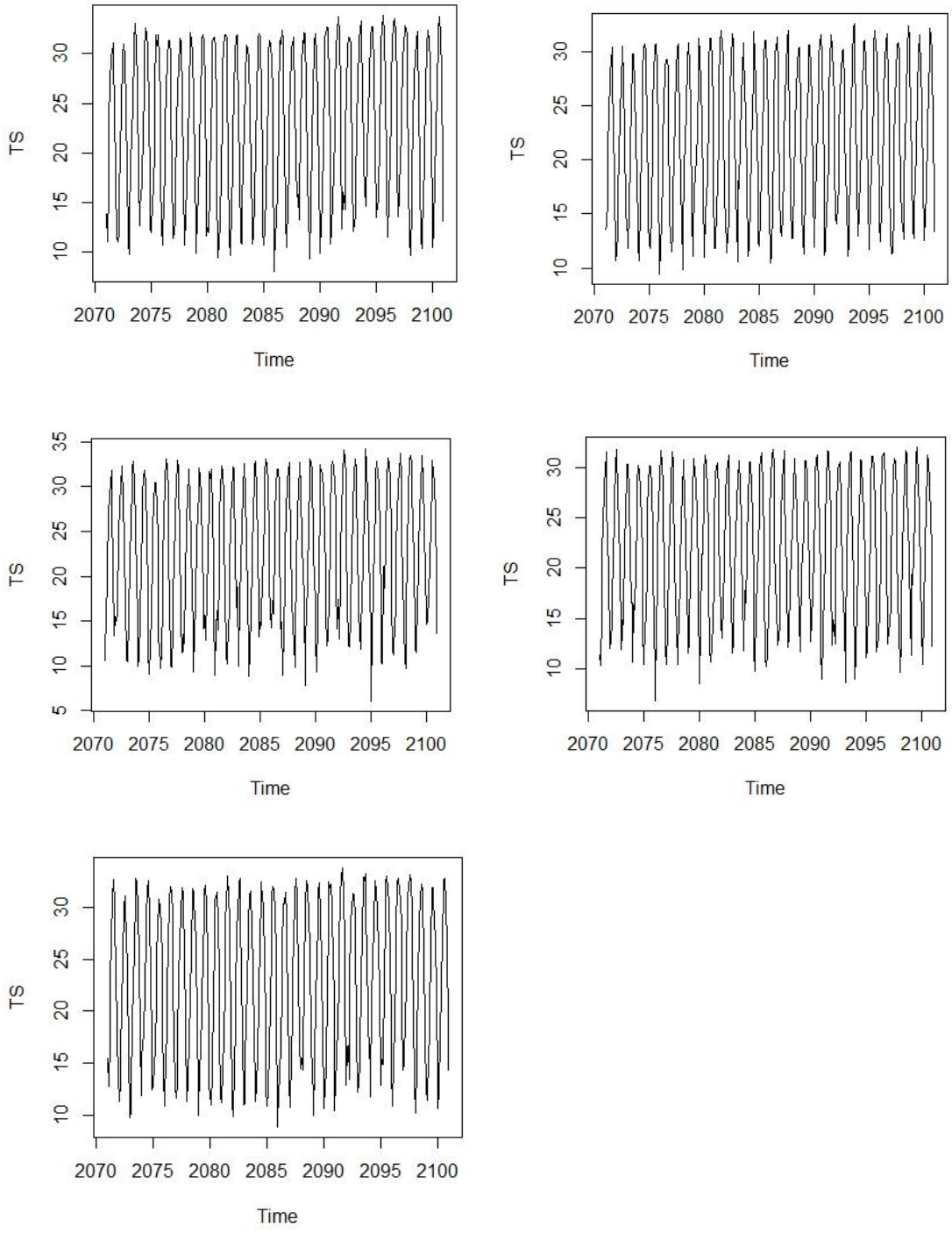

Figure A-5: Temperature trends for 5 CM under MBCn bias correction for RCP 8.5 (2071-2100)

A-2 Changes in hydrological components

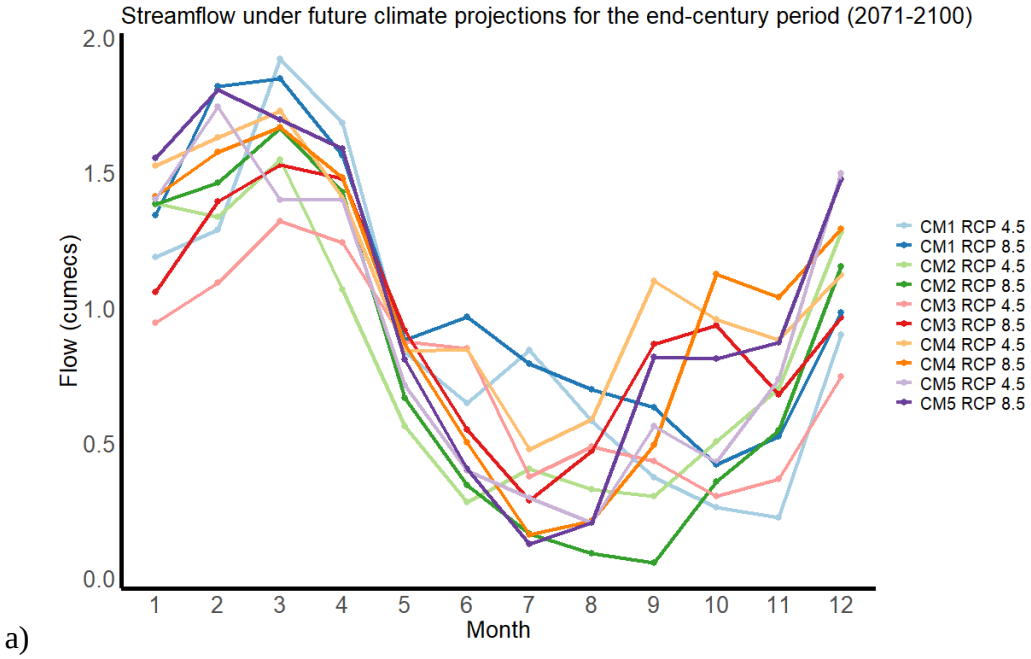

a)

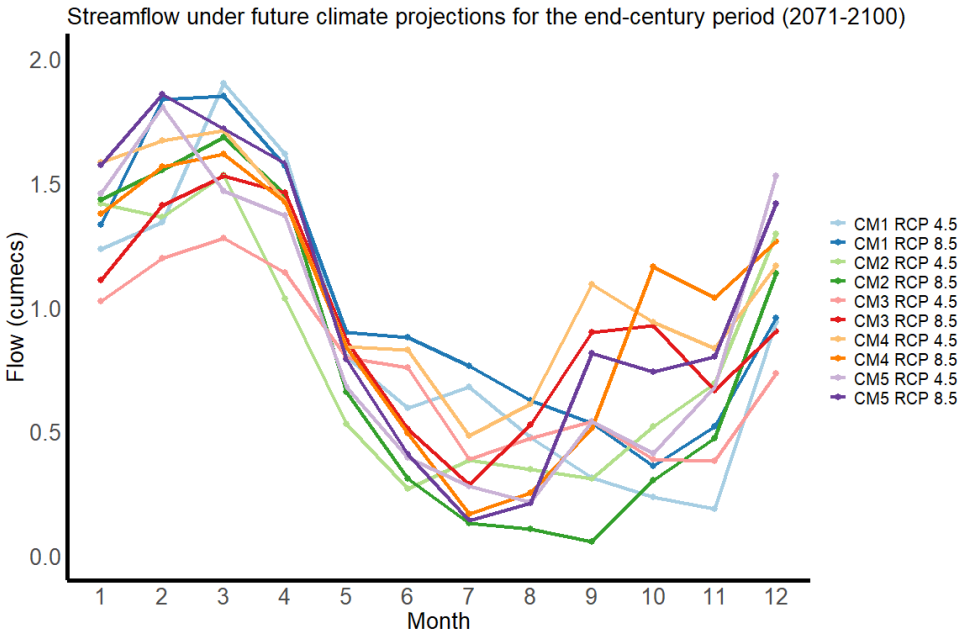

b)

Figure A-6 Monthly streamflow variation (2071-2100) under a) QDM and b) MBCn bias correction methods

Table A-1: Annual water budget for the end century period (2071-2100)

Year	Precipitation (mm)	Surface runoff (mm)	Groundwater (mm)	Evapotranspiration (mm)	Total water yield (mm)
2071	1353.146	366.0552	639.3971	274.0932	1007.084
2072	918.8235	187.2396	408.7688	252.6863	597.0741
2073	963.2385	174.1608	412.6964	274.0932	580.8951
2074	1629.086	502.6212	680.1668	294.0094	1205.728
2075	980.6265	177.3036	653.4847	262.2311	796.3208
2076	1237.572	306.0936	458.8383	274.5852	783.434
2077	1780.286	543.7908	1049.091	281.8274	1575.668
2078	1150.821	262.5696	715.954	268.6369	951.5396
2079	1268.568	358.452	486.332	271.2593	871.2209
2080	1105.745	257.7528	611.8061	248.4944	853.3638
2081	1409.562	369.2196	870.0416	279.1559	1206.138
2082	1311.566	388.5408	523.7583	277.7881	939.6007
2083	1517.67	500.2668	836.5267	278.2703	1335.455
2084	880.173	157.4748	458.4001	255.658	601.8907
2085	1470.798	479.898	590.0254	277.0403	1102.288
2086	1079.757	215.5464	632.2883	254.7182	822.6838
2087	1676.336	559.7964	808.8058	286.4621	1386.836
2088	1416.083	367.794	771.4281	301.3352	1124.808
2089	1765.071	519.9984	1050.341	293.542	1546.18
2090	1377.905	454.4856	862.1051	260.7698	1303.251
2091	1035.437	203.5476	445.1727	273.5864	649.5439
2092	1129.842	267.1056	482.5341	263.1068	755.2776
2093	863.919	129.654	435.6457	252.4255	546.6796
2094	1246.361	357.048	576.7331	276.8582	941.9321
2095	1171.328	261.8568	510.4822	274.7033	774.6335
2096	1255.244	347.7492	672.1979	267.6234	1012.759
2097	1433.66	427.7556	624.5953	276.9911	1071.147
2098	1023.908	188.0604	439.622	276.4548	624.3466
2099	923.265	146.4372	517.9155	279.2002	635.7475
2100	1162.256	299.7756	429.0563	265.9654	750.2433

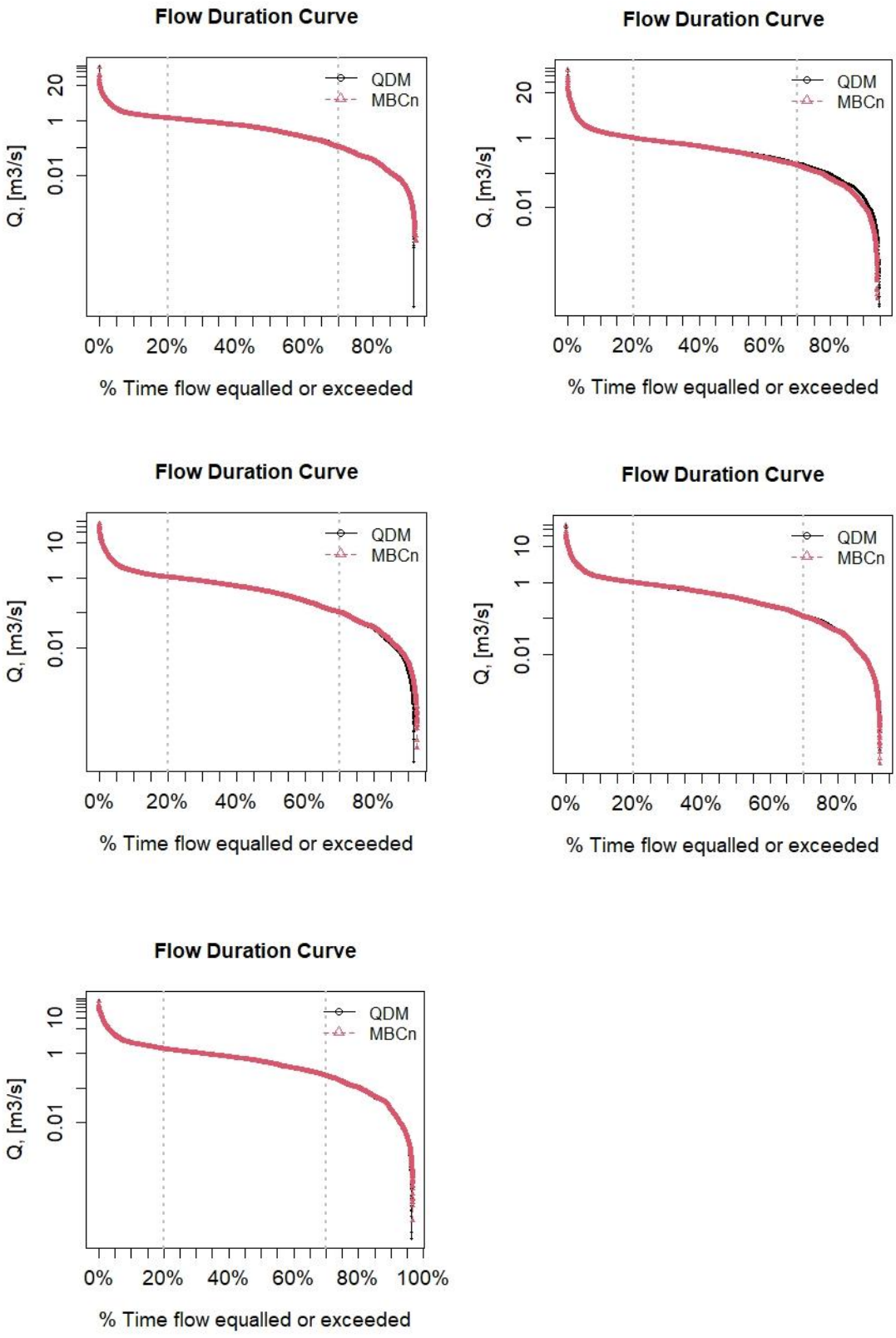

Figure A-7: Flow duration curves for 5 CM under RCP 4.5 scenario (2071-2100)

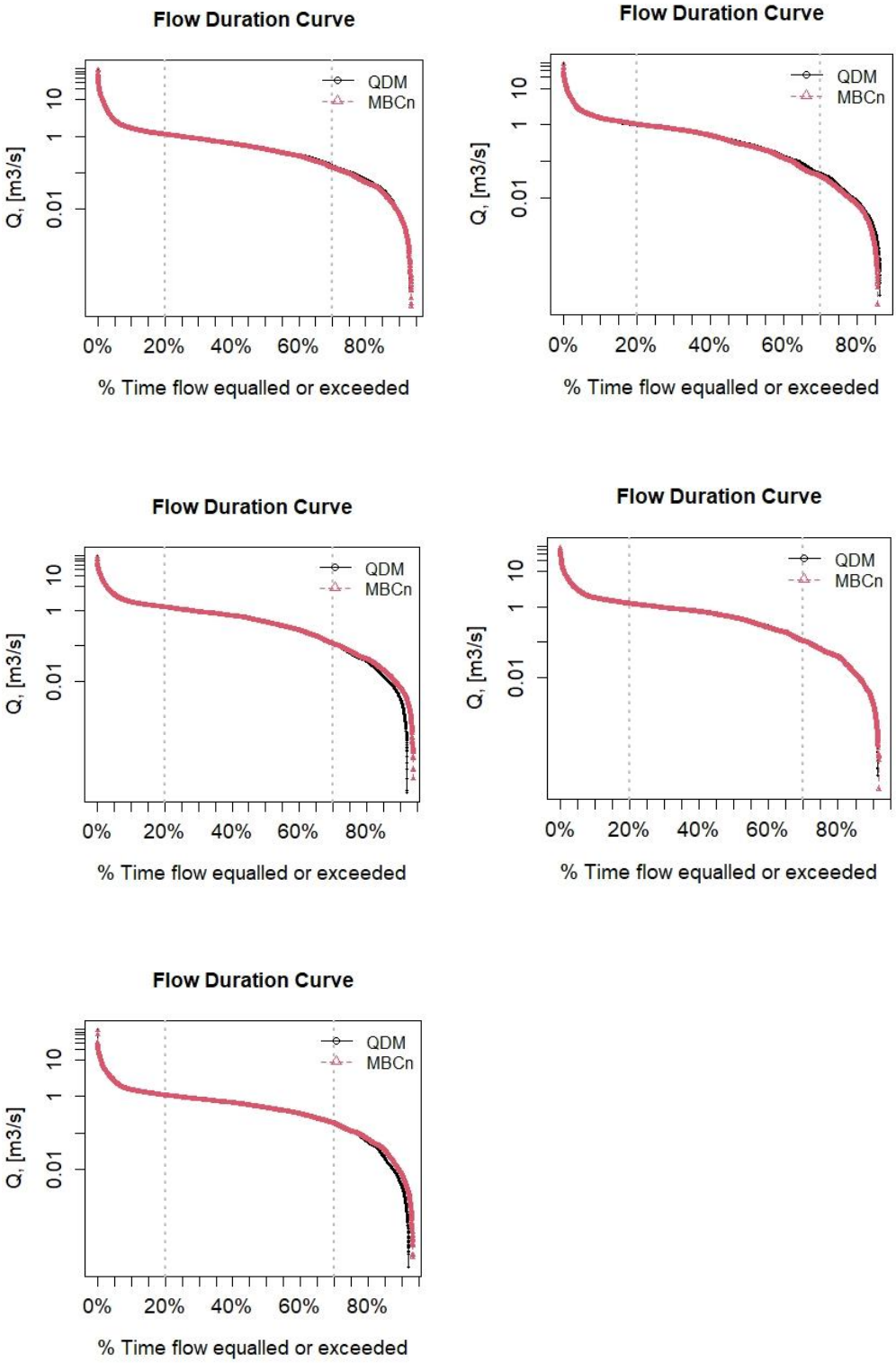

Figure A-8: Flow duration curves for 5 CM under RCP 8.5 scenario (2071-2100)

VITA AUCTORIS

NAME:	Tejith Pogakula
PLACE OF BIRTH:	Hyderabad, India
YEAR OF BIRTH:	1998
EDUCATION:	Sri Venkateswara University College of Engineering, B.Tech., Tirupati, India, 2019
	University of Windsor, M.Sc., Windsor, ON, 2022
EXPERIENCE:	Research Assistant, Dept. of Civil and Env. Engg., University of Windsor, Jan 2020 to Apr 2020
	Graduate Assistant, Dept. of Civil and Env. Engg., University of Windsor, Jan 2020 to Dec 2020